Valorization of the lipid fraction of rice bran via supercritical CO2 and green solvent extraction processes

Applied Food Research 5 (2025) 101285

Contents lists available at ScienceDirect

Applied Food Research

journal homepage: www.elsevier.com/locate/afres

Valorization of the lipid fraction of rice bran via supercritical CO_2 and green solvent extraction processes

Danilo Candela [a], Janine Preston [a,b], Cecilia Fiore [a], Emmanuele Parisi [a], Silvia Fraterrigo Garofalo [a], Francesca Demichelis [a], Debora Fino [a], Elena Simone [a,c,*]

[a] Department of Applied Science and Technology (DISAT), Politecnico di Torino, Torino Italy
[b] School of Chemical and Process Engineering, University of Leeds, Leeds United Kingdom
[c] School of Food Science and Nutrition, University of Leeds, Leeds United Kingdom

ARTICLE INFO

Keywords:
Rice bran
Waste valorization
Lipid extraction
Supercritical CO_2
Life cycle assessment

ABSTRACT

Efficient food resources management, particularly through minimization of waste across the production and supply chain, is essential for creating a resilient, circular agri-food system. The rice industry is one of the largest sectors in agri-food, supporting over half of the global population. This work focuses on valorizing the lipidic fraction of rice bran, a major by-product of rice processing, to contribute to reducing the environmental impact of rice production. Novel purification processes of rice bran wax (RBX) from rice bran are presented, together with their environmental impact assessment. Rice bran butter (RBB) was initially extracted using supercritical CO_2, followed by the separation of its main components, rice bran oil (RBO) and rice bran wax (RBX), through combinations of different physical unit operations including crystallization, centrifugation, solvent extraction and filtration. The purification strategies developed involved green solvents such as ethanol and isopropanol, compared to the commonly used hexane. The purified products were characterized in terms of their chemical properties via chromatographic techniques. Differential Scanning Calorimetry (DSC) and X-ray diffraction were used to determine structural and thermal properties of the material extracted. A Life Cycle Assessment (LCA) was also conducted to determine the environmental impact of the designed extraction and separation processes. The LCA highlighted that the optimal process configuration balances wax extraction yield, energy consumption, and solvent use. Process #2 using ethanol emerged as the most sustainable option, achieving the highest performance with the lowest environmental impact.

1. Introduction

During the last decade, using a Circular Economy (CE) approach in fields such as agri-food has been essential for the development of resilient economic systems focused on waste reduction and valorization (Ghisellini et al., 2016; Kumari et al., 2018). CE strategies focus on moving away from traditional waste management approaches and towards agri-food systems capable of ensuring a balance between environmental, economic and social sustainability (Ghisellini et al., 2016; You, 2022). The agri-food sector generates a significant amount of global waste, with the fruit and vegetable industry alone accounting for an estimated 45 % of the total waste (FAOSTAT, 2019). Reducing this waste could yield major global benefits. Moreover, many agri-food residues can be valorised (e.g., through the extraction of high-value compounds) improving both sustainability and resource efficiency (Bas-Bellver et al., 2020). As a representative recent example, in their work, Bas-Bellever et al., 2020 show how agricultural by-products can be successfully processed to produce new food additives such as natural colourings, preservatives and flavours (Bas-Bellver et al., 2020).

In this work we focused on rice bran (RB), a by-product generated from rice processing, one of the largest global agri-food sectors (Mohidem et al., 2022; Nikitha & Natarajan, 2020) on which about half the global population depends (Tan et al., 2023). RB is the outer layer of the rice grain, it accounts for approximately 10 %wt of the non-consumed rice portion (Mohd Esa & Ling, 2016; Sapwarobol et al., 2021) and contains a wide range of added-value molecules that could be isolated and valorized (Butsat & Siriamornpun, 2010; Yu et al., 2007). These are lipophilic compounds such as tocopherol, tocotrienol and γ-oryzanol that have antioxidant properties and may help in the prevention of cardiovascular system related diseases (Min et al., 2011;

* Corresponding author.
E-mail address: elena.simone@polito.it (E. Simone).

https://doi.org/10.1016/j.afres.2025.101285
Received 15 April 2025; Received in revised form 22 July 2025; Accepted 24 August 2025
Available online 26 August 2025

Mohd Esa & Ling, 2016). It is also known that the amount of γ-oryzanol in RB is up to five times higher than in other by-products of the rice industry (Yu et al., 2007). Furthermore, RB contains many other useful food nutrients such as proteins, dietary fibres and fats (Fraterrigo Garofalo et al., 2021). The lipid fraction is one of the most abundant in RB, and it is extracted and commercially traded especially in Asian countries (Nikitha & Natarajan, 2020; Rohman, 2014). This product is usually called rice bran oil, and it contains about 3–5 % of the antioxidant molecules mentioned above (Singanusong & Garba, 2019). Significant research has focused on extracting, characterizing, and designing novel food products using the rice bran lipid fraction (Fraterrigo Garofalo et al., 2023; Tan et al., 2023). Its nutritional (Sahini & Mutegoa, 2023) and stabilizing benefits (Kim & Godber, 2001; Nanua et al., 2000) as a food additive have been demonstrated in several studies. However, the current techniques for extracting the lipid fraction of rice bran present many technological and environmental limitations (Sahini & Mutegoa, 2023). The most common techniques involve the use of organic solvents such as hexane, or hydraulic pressing (Garba et al., 2019; Kordsmeier et al., 2015); however, hexane is a flammable and toxic solvent whereas mechanical pressing delivers low extraction yields. More recently, the development of greener techniques has led to more sustainable processes (Fraterrigo Garofalo et al., 2021; Garba et al., 2019). Some of these involved the use of green solvents such as ethanol, isopropanol, and d-limonene. However, depending on the conditions used, ethanol and isopropanol may lead to lower yields of extracted RBO compared to hexane (Ruen-Ngam, 2014). On the other hand, d-limonene has an evaporation temperature of 176°C, making it unfeasible to recover RBO from this solvent for energy consumption reasons (Liu & Mamidipally, 2005). Other studies focused on the potential of using supercritical CO_2 ($SCCO_2$) for RBO extraction. In this regard, Fraterrigo Garofalo et al., 2023 designed a $SCCO_2$ extraction method for the recovery of rice bran oil from RB residues, using a multi-factorial design of experiment approach (Fraterrigo Garofalo et al., 2023). The influence of varying pressure and temperature was also underlined by Tomita et al., 2014. In their work, they focused on the effect of these two process parameters on the solubility of RBO in $SCCO_2$, findings that an increase in pressure has a more significant effect compared to increasing temperature (Tomita et al., 2014). By optimizing the process conditions, a $SCCO_2$ extraction can lead to similar yields compared to common hexane Soxhlet extraction. Nevertheless, hexane is not a generally recognized as safe (GRAS) solvent, making the extracts obtained with $SCCO_2$ extraction safer for human health (Kuk & Dowd, 1998). Before it can be used for human consumption, rice bran oil requires a refining process due to a significant presence of compounds such as free fatty acids, polar lipids, non-saponifiable components and waxes (Tufail et al., 2024). Rice bran wax (RBX) has recently emerged as a valuable excipient for cosmetic, pharmaceutical and food formulations (Vali et al., 2005). The lack of standard methods for its chemical analysis led to the difficulty to determine the exact composition or rice bran wax (Vali et al., 2005); although, it is known that some of its main components are polycosanols (Ishaka et al., 2014; Pandolsook & Kupongsak, 2020). These molecules with long carbon chains have been shown in many studies to be useful for the treatment of gastrointestinal disorders, such as gastric and duodenal ulcers (Carbajal et al., 1995; Ishaka et al., 2014). Despite its significant added value, the isolation and purification of RBX from RB is still a complicated process for which there is no standard procedure (Vali et al., 2005): this limits its commercial availability and applications. In general, RBX is extracted using winterization techniques, followed by centrifugation and filtration (Ishaka et al., 2014; Modupalli et al., 2022; Strieder et al., 2017). However, these methods have proved to be ineffective in obtaining very pure RBX that could be used in highly regulated products such as pharmaceutical formulations (Strieder et al., 2017; Vali et al., 2005). Nevertheless, numerous studies have been conducted with the aim of understanding how RBX can be employed effectively in formulation design. For instance, Dassanayake et al. (2009) have investigated the dynamics of organogel formation employing several types of liquid oils and RBX as gelling molecule (Dassanayake et al., 2009).

Since the present study adopts alternative extractive and purification methods compared to those currently used, it is important to study the environmental impact associated with the proposed process. One of the most adopted tools to quantify the environmental impact of a process or a product is the Life Cycle Assessment (LCA) according to ISO 14040–44. In scientific literature, several environmental studies are available about rice, such as the ones concerning a Chinese case study about rice bran oil extraction (L. H. Sun et al., 2022), the extraction of rice bran oil through alternative extraction techniques, (Fraterrigo Garofalo et al., 2022) and an environmental review study about rice by-products conversion into high added value products (Sanoja-Lopez et al., 2024). However, no environmental studies about wax extraction from rice bran are currently available in the literature.

The purpose of this work is to explore novel processes for the isolation and purification of RBX from rice bran and to assess their environmental impact. Given the lack of standardized protocols in the current literature, this work aimed to develop sustainable and reproducible methods to isolate RBX with high purity using green technologies. Initially, RB was processed through $SCCO_2$ extraction in order to recover its lipid fraction. CO_2 has a low critical pressure and temperature under supercritical conditions, which can be reached with standard pumping equipment (Sahena et al., 2009). Additionally, this solvent is safe and easy to separate from the lipid extract. The extracted lipid fraction was characterized in terms of its chemical, thermal and structural properties. This was followed by the development of five different strategies for the purification and isolation of RBX from the lipid extract. The proposed processes were designed using combinations of unit operations, including centrifugation, solvent extraction and filtration. A life cycle assessment was conducted to estimate the environmental impact of the developed sequences of unit operations. Finally, after identifying the most favourable and sustainable process, the structural characteristics of RBX were further investigated in more detail. The RBX structural characterization confirmed the prevalence of a several solid phases characterized by orthorhombic sub-cells (Pandolsook & Kupongsak, 2020).

2. Materials and methods

2.1. Rice bran matrix characterization

Samples of ground rice bran with a particle diameter of 500 μm were kindly provided by Agrindustria Tecco S.R.L. and stored at -20°C until use. The matrix was characterized by determining its moisture, proteins, lipids, and ashes content. These measurements were performed in triplicate.

2.1.1. Moisture content

The "Analytical methods used in food control" (ISTISAN reports 96/34) protocol established by the Istituto Superiore di Sanità (Baldini et al., 1996) was used to conduct the moisture content analysis. A crucible was filled with 5 g of rice bran and dried overnight at 103°C in a MEMMERT UN 30 air stove manufactured by Vetrotecnica (Italy). The test was conducted in triplicate. The moisture percentage was calculated as follows:

$$\%Moisture = \frac{w_{in} - w_{dried}}{w_{in}} \quad (1)$$

where w_{in} is the initial weight of the sample before drying and w_{dried} is the weight of the sample after drying. The dried matrix was used for the measurement described below.

2.1.2. Protein content

The protein content of rice bran was estimated using the Dumas

method (Serrano et al., 2013). The protocol is divided into three steps (combustion, reduction and separation, and detention) after which the total nitrogen (%*N*) content is quantified. The analysis was conducted using an elemental analyzer MacroCube purchased by Elementar Italia Srl (Italy). The total percentage of protein was calculated using the following relation:

$$\%Protein = 5.34 \cdot \%N \quad (2)$$

where 5.34 is a correction factor normally used for cereals (Mariotti et al., 2008).

2.1.3. Lipid content

The quantification of the lipid percentage was performed in accordance with the "Analytical methods used in food control" (ISTISAN Reports 96/34) protocol established by the Italian Istituto Superiore di Sanità (Baldini et al., 1996). The lipid content was isolated using a Soxhlet extractor. Around 2 g of dried rice bran were placed in the extraction chamber into a thimble filter with an equal amount of anhydrous sodium sulphate Na_2SO_4, to remove any eventual traces of moisture. The filter was sealed with a degreased cotton swab. The extraction was conducted for 8 hours using petroleum ether. The extract was collected in a flask and distilled to separate it from petroleum ether. The residue was left to dry in stove. After being cooled in a drier, it was weighted, and the percentage of lipids was estimated as following:

$$\%Lipids = \frac{w_{ext}}{w_{in}} \cdot 100 \quad (3)$$

Where w_{ext} is the weight of the extracted sample and w_{in} is the initial weight of the rice bran before the extraction.

2.1.4. Ashes content

The ashes content was calculated in accordance with the "Analytical methods used in food control" (ISTISAN Reports 96/34) established by the Italian Istituto Superiore di Sanità (Baldini et al., 1996). The samples were incinerated in a muffle at 550°C. The heating ramp used was 2°C/min. The process was carried out in 8 hours after which, samples were left cooling and then weighted. The total percentage of ashes was estimated as follow:

$$\%Ashes = \frac{w_r}{w_{in}} \cdot 100 \quad (4)$$

where w_r is the weight of the incinerated sample and w_{in} is the initial weight of the rice bran sample processed.

2.2. Supercritical CO_2 ($SCCO_2$) extraction of rice bran butter (RBB) from rice bran

The extraction of the lipid fraction of rice bran (rice bran butter, RBB) was conducted at Exenia Group S.r.l in Pinerolo (Italy) [4]. The schematic representation of the system is presented in Fig. 1. A closed cycle of 250 kg of CO_2 was used for each extraction, which lasted 4 hours. CO_2 was selected as the supercritical fluid due to its strong affinity for lipidic compounds during extraction and its suitability for food-grade applications (Sookwong & Mahatheeranont, 2017). Rice bran was first dried overnight at 70°C in a Nerone oven (Tecnodom), after being placed in flat trays. Afterwards, 4 or 5 kg of dried RB were loaded in a 20 L cylindrical extractor and mixed with metal Raschig rings that enabled uniform distribution of the RB powder within the extraction chamber and ensured that the CO_2 did not flow through preferential paths during extraction operation. $SCCO_2$ was continuously fed into the extractor during the 4-hour process. The pressure of $SCCO_2$ within the extractor was 330 bar, with a temperature of 60°C. Since the extraction took place at the pilot plant of the industrial partner, the operational conditions were those routinely applied in their system and could not be independently modified during the trials. In the downstream section of the extractor, a lamination valve was placed to reduce the pressure and enable the return of the CO_2 to the gaseous state. Following that, a gravimetric separator operating at 150°C equipped with a nozzle was placed for the separation of CO_2 from the extracted product. In the end, the RBB extracted was fed through two cyclonic separators operating at 2–3°C to collect any residual water or solvents. After all the operations, the RBB was stored at 4°C to prevent possible alterations.

2.3. Fatty acids (FA) characterization of RBB

The fatty acid (FA) composition of RBB was determined according to the standardized protocols UNI EN ISO 12,966–2:2017 (International Organization for Standardization, n.d.-b) and UNI EN ISO 12, 966–4:2015 (International Organization for Standardization, n.d.-a). The FAs were analyzed as fatty acids methyl esters (FAME) using a GC Agilent 7890A gas chromatograph (Agilent, USA) equipped with a

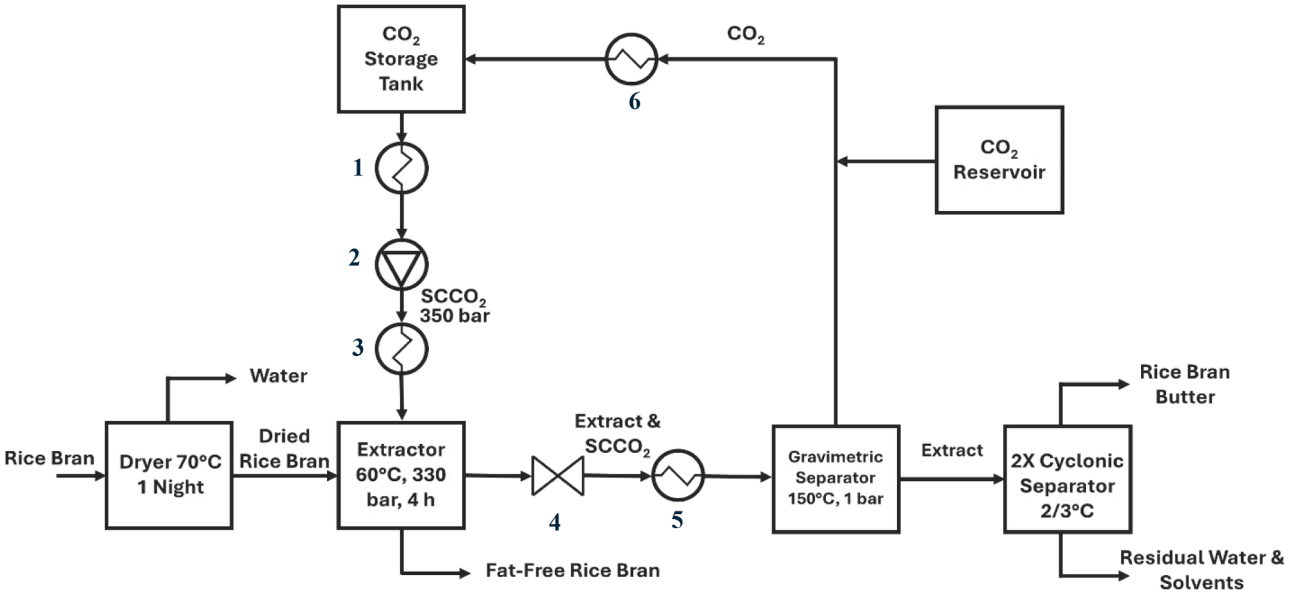

Fig. 1. Scheme of the $SCCO_2$ extraction plant located at the Exenia Group S.R.L. facilities. Process diagram adapted from Fraterrigo Garofalo et al. (2023). Legend: 1) Heat exchanger, 2) Diaphragm pump, 3) Evaporator, 4) Throttling valve, 5) Heat exchanger, 6) Condenser.

ZB-FAME column (30 m × 0.25 mm ID × 20 μm; Zebron Phenomenex, USA) and a quadrupole mass detector Agilent 5975 C VL MSD (Agilent, USA). FAME were prepared by dissolving 100 mg of RBB in 3 ml of methanolic KOH (0.6 M) (Merck, Germany) in a Falcon tube and shaken for 10 s under a stream of N_2 to prevent oxidation of the compounds. The solution was then heated at 70°C for 10 min in a water bath under agitation. Once the oil was completely dissolved, 3 ml of H_2SO_4 5 % (Merck, Germany) were added, and the solution was heated to 70°C for a further 5 min. Then, 2 ml of a saturated NaCl solution (Merck, Germany) and 2 ml of hexane (Merck, Germany) were added, and the Falcon tube was centrifuged at 4000 rpm for 10 min with an SL16R centrifuge (Thermo Fischer, USA). The supernatant was collected, diluted with hexane with 1:2 ratio and transferred into a vial for GC–MS analysis. Helium was used as carrier gas with a flow rate of 0.4 ml/min, the injection volume was 1 μl using split mode with a split ratio of 20:1 at 240°C. The injector temperature was kept instead at 250°C. The column was initially set at 100°C for 2 min and then the temperature was increased to 240°C with a ramp of 5°C/min. This temperature was held constant for a further 8 min. The mass analyzer operated in electron ionization mode with an ionization energy of 70 eV and in full scan mode between 50 and 600 a.m.u.. The source and quadrupole temperatures were respectively maintained at 230°C and 150°C. The FAME quantification was determined by using calibration curves prepared using a standard FAME mixture and using OpenLab ChemStation software (Agilent, USA) and the NIST08 Library (National Institute of Standards and Technologies, USA).

2.4. Triacylglycerides (TAGs) characterization of RBB

A gas chromatographic (GC) analysis was performed to determine the triglycerides present in the RBB. This analysis was performed using a polar gas chromatography column RTX-65 (65 % diphenyl-35 % dimethyl polysiloxane), length 30 cm, internal diameter 0.25 mm and film thickness 0.10 μm. The single triglycerides were separated according to the number of carbon atoms and the degree of unsaturation of the glycerol-bound fatty acids. The identification of the individual components was performed based on gas chromatographic retention times with respect to a certified reference material (cocoa butter IRMM-801). The test sample was melted in an oven at 80°C, diluted in isooctane to a concentration of approximately 0.1 mg/ml and injected into the gas chromatography system. The GC/FID analysis was performed using an Agilent mod. 7890 B gas chromatograph equipped with a flame ionisation detector (FID). The analysis was conducted using on-column injection. The carrier gas used was helium at a constant 3 ml/min flow rate. The oven temperature was set at 60°C for one minute. Then, the temperature was increased to 300°C with a 20°C/min ramp. Subsequently, a temperature of 365°C was reached using a 5°C/min ramp and this temperature was maintained for 8.5 min. The FID detector working temperature was 370°C.

2.5. RBB fractionation and purification

RBB samples were initially centrifuged through a Thermo ScientificTM SL16 centrifuge, commercially available from Fisher Scientific (USA). The samples were first heated to 40°C in a water bath and then placed in a centrifuge operating at the same temperature. A semi-solid fraction and a liquid fraction were obtained after centrifugation at 5000 rpm for 20 min. To further purify this semi-solid phase, rich in RBX and other saturated TAGs, it was heated up to 50°C and kept for a few hours in a 200 ml jacketed reactor connected to a Huber Ministat 230 (Germany) thermoregulator. Subsequently, the sample was vacuum filtered (360 mbar) using qualitative filter paper Whatman® Grade 4 and a Vacuum Pump SC9204 commercially available from KNF (Germany). After filtration, the filter cake was washed with ethanol to further remove the residual oil. The centrifuged only sample, the centrifuged and filtered sample, and the centrifuged, filtered and washed with ethanol sample were then analysed for their thermal and structural properties without further processing.

Five purification processes involving the use of organic solvents and starting from RBB were developed. The complete process diagrams with relative process conditions are shown in detail in Supporting Information Figures S1-S %. The first step employed in every strategy was the melting of RBB in a Thermostatic Stove (Memmert Standard Series, Germany) at 80°C for one hour. After a vigorous hand mixing to guarantee sample uniformity, about 25 ml of the molten RBB were used for each purification process tested. The centrifugation and filtration steps were carried out with the same equipment and setups described earlier, but with different operating conditions as reported in the process diagrams. Centrifugations were always carried using 5000 rpm and 40°C as speed and temperature, the highest values reachable for this type of equipment. The duration of the centrifugations was adapted each time by looking at the degree of separation observed in the Falcon tubes. Filtrations were always carried out using 200 mbar as set-point. Preliminary trials revealed that employing a lower pressure did not result in any specific advantage. Absolut ethanol (EtOH) or isopropanol 99.8 % pure (IPA), purchased from Sigma-Aldrich, were both tested as solvents for enhance the extraction in each purification strategies. The selection of these two solvents was determined by their low boiling point, cost-effectiveness and ease of handling in laboratory and industrial settings, in comparison to alternative green solvents such as limonene (Liu & Mamidipally, 2005) or ethyl lactate (Pereira & Rodrigues, 2014).

2.5.1. Process #1

Process #1 is presented in **Figure S1 of Supporting Information**. After being melted, RBB was centrifuged twice (the first one without the aid of the solvent, the second one with the help of the solvent) to isolate its high melting fractions. The precipitate obtained was then molten again, other solvent was added, and another centrifugation step was performed. As shown in the process diagram, the steps of melting, adding solvent, and centrifuging were repeated another time. Finally, a vacuum filtration was performed to isolate RBX.

2.5.2. Process #2

Process #2 is similar to Process #1 and presented in **Figure S2 of Supporting Information**. This process is distinguished by the inclusion of an additional melting and solvent addition step after the first centrifugation. Furthermore, the two following centrifugations were performed with increased centrifugation times (respectively 25 min and 45 min). Concerning all the other unit operation steps employed, they remained unchanged in sequence order, type and operating conditions.

2.5.3. Process #3

The schematic representation of Process #3 is shown in **Figure S3 of Supporting Information**. It includes only a first centrifugation step of 30 min, followed by a subsequent vacuum filtration. This final step is performed adding hot solvent at 60°C. It is the shortest purification strategy used among the five developed.

2.5.4. Process #4

Process #4 is presented in **Figure S4 of Supporting information**. After the first centrifugation step of 30 min, the precipitate was molten, and 5 ml of solvent were added (larger amount compared to Process #1 and #2). Another centrifugation of 30 min, followed by another additional melting and solvent addition step, was performed. Comparing with the other processes presented so far, the final vacuum filtration was not preceded by a final centrifugation.

2.5.5. Process #5

The process diagram of Process #5 is represented in **Figure S5 of Supporting Information**. After the first centrifugation of 30 min, the precipitate recovered was melted at 90°C and 10 ml of warm solvent (at 50°C) for each gram of sample were added. The mixture was then stirred

at 50°C for 20 min. A winterization step of 36 hours at 4°C was performed, followed by a final vacuum filtration to isolate the solid fraction.

2.6. Recovery of rice bran oil (RBO) and organic solvents

All liquid oil fractions obtained from the five purification processes were collected at the end of each purification step. This liquid fraction was characterized by the liquid component of RBB, the rice bran oil (RBO) and the organic solvents EtOH and IPA. The RBO and solvents were separated using a Hei-VAP Core evaporator connected to a Vacuum Controller Hei-VAC Control and a Vacuum Pump Hei-VAC Valve Tec (Heidolph Scientific Products GmbH, Germany). The process temperature and pressure were 50°C and 75 mbar, and the time of processing was 20 min.

2.7. Differential scanning calorimetry (DSC)

Differential Scanning Calorimetry was used to assess the purity of the samples after the different processing steps. Heat flow measurements were performed using a Mettler Toledo DSC 1 (Mettler Toledo, USA). Each sample was weighed and sealed in an aluminium pan, while an empty aluminium pan was used as the reference. The unprocessed and fractionated RBB samples were taken with a spatula and put in the pan up to a weight of around 6 mg and were heated from -40°C to 100°C at a rate of 5°C/min, then cooled down back to -40°C at a rate of -2°C/min. For RBX samples, each sample was manually grinded and then placed in the pan up to a weight of around 3 mg and was heated from 25°C to 100°C at a rate of 5°C/min, then cooled to 10°C at a rate of -2°C/min. The measurements were conducted in N_2 rich environment with a flow of 50 ml/min.

2.8. Synchrotron X-Ray diffraction

The nano and sub-nanostructural analysis of RBB fractions and purified RBX were conducted using the SAXS beamline at Elettra Sincrotrone Trieste (Italy) and the I22 beamline at Diamond Light Source (DLS, UK). At Elettra a Pilatus3 1 M detector (Dectris DH, Switzerland) was used to detect the SAXS signal (range = $0.76 < q < 57.5$ Å^{-1}) while a Pilatus 100k detector was used for the analysis of the WAXS region (range = $63 < q < 163$ Å^{-1}); the beam energy was 8 keV (1.54 Å wavelength). At DLS a Pilatus P3–2 M from Dectris was used as SAXS detector, whereas for WAXS a Pilatus3–2M-DLS-L detector was installed. The beam energy used at I22 was 18 keV. For all samples and synchrotron setups calibration was performed with silver behenate (d-spacing 58.38 Å) for the SAXS region and p-bromobenzoic acid for the WAXS region. A quartz capillary with a diameter of 1.4±0.1 mm and a length of approximately 80 mm was used as the sample holder. An empty capillary of the same size was used as the reference. The capillaries were filled with melted samples using a syringe equipped with 120 mm long needle and, after being placed in the set-up, were heated to 70°C, then cooled to 20°C and held at this temperature for two hours. Then, the temperature was increased to 25°C at a rate of 1°C/min, held for 15 min and then set back to 20°C, where it was kept for at least another hour. The scattering patterns obtained were analysed using Origin 2022 software. Peak values were obtained using the *Peak Analyser* embedded Origin function, and d-spacing were calculated according to the Bragg law.

2.9. Powder X-Ray diffraction (PXRD)

PXRD diffractograms of rice bran extracted materials samples were collected using an Empyrean diffractometer (Malvern Panalytical, UK). A CuKα radiation at a wavelength of 1.54 Å was used to record the diffraction patterns between 4–40 2θ degree, with a step size of 0.01313° and time per step of 60 s. RBX samples were ground by hand using an agate mortar and subsequently placed onto a Si zero background and measured without spinning in Bragg Brentano geometry. The X-ray generator was set at a tube voltage of 40 kV and a current of 40 mA. instrument worked at an intensity of 40 mA and a voltage of 40 kV. The further indexing of the relative peaks was conducted with the program *X-Cell* (Neumann, 2003).

2.10. Polarized light microscopy (PLM)

RBX samples were visually analysed using optical PLM. Approximately one flake of each RBX sample from the purification processes tested was transferred on a glass slide and then covered with a cover glass. The glass slide was placed on a Linkam PE120 hot stage, connected to a water circulation pump (Linkam Scientific Instruments, UK). The hot plate was positioned on a Zeiss Axiolab 5 microscope (Zeiss, Germany) with a polarized light lens. The temperature was then controlled with a T96 Peltier LinkPad controller. Each sample was heated from 25°C to 80°C at 5°C/min, then cooled down to 10°C at -2°C/min as these were also the ramp used during the DSC analysis. Pictures of the RBB and RBX crystals were taken with a Samsung Galaxy A51 (Samsung, South Korea), using the 10X and the 40X magnification lens of the microscope. Images were then processed using ImageJ 1.54d software (USA) to add the scale.

2.11. Life cycle assessment

The Life Cycle Assessment (LCA) was performed with SimaPro 9.5.0.2 software and the Ecoinvent 3.8 database, in compliance with ISO 14,040–14,044 (2006). The study aimed to quantify the environmental impact of the five purification processes described above for converting rice bran (RB) into rice bran wax (RBX) as the primary product, and rice bran oil (RBO) as a co-product. The two organic solvents considered were ethanol and isopropanol.

The scope of the study was to identify the processes' hotspots and propose improvements for environmentally efficient wax recovery. Since the target product is the high-value RBX, the functional unit (FU) was defined as 1 kg of RBX produced per year. This amount was selected based on the RB availability in the Italian region of Piedmont, the capacity of the $SCCO_2$ extraction plant to produce RBB even in the lowest-yield configurations, and to address the wax market demand. Our decision to conduct LCA also at a relatively low scale was motivated by the fact that an analysis at industrial scale (FU = 1 kg of RBX produced per year) was already performed by Piccinno et al. (2016). LCA can help in understanding the laboratory process from an environmental perspective, but it gives a limited indication of the possible environmental impact; hence, LCA of an industrial scale is usually preferable. In the present study, the key assumption for going from laboratory to industrial production included no scale effect on the extraction and separation efficiencies; this is reasonable, as all processes are physical transformations.

Additionally, our study was geo-contextualized in Piedmont, located in northwestern Italy, where the $SCCO_2$ extraction production plant is located. Following the "grave-to-gate" approach (Thushari et al., 2020), the analysis encompassed processes from rice bran conversion at the extraction plant to the production of market-ready wax and oil. Transportation of raw materials and transportation and distribution of the market-ready wax and oil were excluded, as the study focused on comparing different purification processes.

The LCI for the five configurations is summarized in **Table S1–10**. LCI includes Exenia Group's RBB production steps (drying, extraction, and cyclonic separation) and the subsequent purification processes. Each configuration was analyzed considering the use of ethanol (denoted as configuration A) and isopropanol (denoted as configuration B) as solvents. Although the base process for RBB production was consistent across configurations, variations in rice bran input quantities influenced the daily cycle requirements to meet the target of 1 kg/year RBX. Primary data for the LCI were obtained from experimental tests described

in the previous sections and scaled up according to the selected FU. Solvent recovery rates of 90 % were assumed, based on (Perry & Green, 2008) and (Protection Agency, 2010). This assumption was made to align the investigated process more closely with real industrial conditions. However, it does not influence the LCA results, as the same solvent recovery rate was assumed for both solvents. The environmental impacts associated with solvents depend primarily on the type of solvent and the quantity used in each process configuration. The zero-burden concept was considered by attributing no environmental credits to rice bran for prior life cycle stages. The energy consumption of laboratory equipment such as centrifuges (*Lehmann Industrie - Top Discharge Vertical Centrifuges*, n.d.) and rotavapors (ZHENGZHOU GREATWALL Scientific Industrial and Trade Co., Ltd. - 10L Rotary Evaporator) was based on technical commercial setups. The considered energy mix was the Italian one. LCA is a geo-referenced study; it is important to consider the energy mix of the selected country. However, the choice of the energy mix is not particularly significant in this study, because all 10 configurations have been analysed under the same boundary conditions and energy mix. For this reason, one limitation of our approach is that it cannot be compared directly with the same study performed using a different country mix.

The system was divided into foreground and background components, following Clift et al. (2000). The foreground system considered processes directly managing the reference flow, while the background system accounted for related activities such as energy production, chemical supply, and avoided products. Attributional LCA was performed, and multi-output products were managed using economic allocation consistent with ISO 14,040–44. Fat free rice bran and RBO, treated as co-products, were allocated based on economic value, with prices derived as follows: RB ((*Rice Bran Butter*, 2025)), fat free rice bran (*Feed Prices and Markets*, 2025), RBX (*Rice Bran Wax, 500 g High Hardness, Excellent Miscibility*, 2025), and RBO (*Rice Bran Oil*, 2025) and reported in Table 1. Usually, LCA ISO 14,040–44 suggests the use of mass allocation. However, the use of economic allocation is also supported by studies such as (Beccali et al., 2010) on citrus processing and (Cherubini et al., 2011) on lignocellulosic biorefineries, both of which applied economic allocation in contexts like the one of the present study. These studies argue that when co-products have markedly different economic values compared to their mass (e.g., essential oils versus pulp), economic allocation provides a more appropriate and representative distribution of environmental impacts.

In the present study, economic allocation was preferred over mass allocation because RBX represents the limiting product in terms of quantity across all five purification techniques, accounting for approximately 0.2–0.8 %w/w of the total products obtained (RBX and RBO). Additionally, RB, fat free rice bran, RBX, and RBO have market demands, making economic allocation a more relevant approach to reflect the economic context of these co-products. Since the market value of the primary product is significantly higher than that of the by-products, Batuecas et al. (2019) stated that impact should not be distributed based on the physical properties of the products, as this could result in an unfair burden allocation among lower-value co-products. Similarly, Gabisa et al., 2019 emphasized that economic allocation helps decision-makers identify the most economically viable use of co-products. Table 1 summarizes the economic allocation method and highlights its differences from mass allocation, highlighting why the latter was not selected.

The Life Cycle Impact Assessment (LCIA) was performed with the ReCiPe 2016 Midpoint (H) method implemented in the SimaPro software. A final LCA step was design to interpret the results and identify the purification process with the lowest environmental impact; a sensitivity analysis evaluated the robustness of impact trends across methodologies. Specifically, the consistency of the results was proven through

Table 1
Details about the LCA based on economic allocations. The mass allocation is not considered but reported to underline that RBX would be underestimated with mass allocation.

					Allocations	
		Quantity (kg/y)	Price (euro/kg)	Revenues (euro)	Economic (%)	Mass (%)
RB production	Rice bran butter	0.29	12.66	3.67	52.18	2.53
	Fat free rice bran	11.18	0.301	3.37	47.82	97.47
	Total	11.47	12.96	7.04	100.00	100.00
1A-	RB_wax	1.00	35.95	35.95	16.47	0.47
	RB_oil	211.88	0.86	182.29	83.53	99.53
	Total	212.88		218.24	100.00	100.00
1B	RB_wax	1.00	35.95	35.95	15.42	0.43
	RB_oil	229.28	0.86	197.26	84.58	99.57
	Total	230.28	36.81	233.21	100.00	100.00
2A	RB_wax	1.00	35.95	35.95	23.01	0.71
	RB_oil	139.81	0.86	120.29	76.99	99.29
	Total	140.81	36.81	156.24	100.00	100.00
2B	RB_wax	1.00	35.95	35.95	20.06	0.60
	RB_oil	166.56	0.86	143.29	79.94	99.40
	Total	167.56	36.81	179.24	100.00	100.00
3A	RB_wax	1.00	35.95	35.95	9.14	0.24
	RB_oil	415.31	0.86	357.30	90.86	99.76
	Total	416.31	36.81	393.25	100.00	100.00
3B	RB_wax	1.00	35.95	35.95	8.07	0.21
	RB_oil	475.79	0.86	409.34	91.93	99.79
	Total	476.79	36.81	445.29	100.00	100.00
4A	RB_wax	1.00	35.95	35.95	12.80	0.35
	RB_oil	284.76	0.86	244.99	87.20	99.65
	Total	285.76	36.81	280.94	100.00	100.00
4B	RB_wax	1.00	35.95	35.95	15.28	0.43
	RB_oil	231.60	0.86	199.25	84.72	99.57
	Total	232.60	36.81	235.20	100.00	100.00
5A	RB_wax	1.00	35.95	35.95	20.76	0.62
	RB_oil	159.47	0.86	137.20	79.24	99.38
	Total	160.47	36.81	173.15	100.00	100.00
5B	RB_wax	1.00	35.95	35.95	22.26	0.68
	RB_oil	145.93	0.86	125.54	77.74	99.32
	Total	146.93	36.81	161.49	100.00	100.00

sensitivity analysis by varying the RBX yields about − 5% w/w according to Demichelis et al. (2022).

3. Results and discussion

3.1. RB characterization

The RB chemical characterisation results are shown in Table 2. As described in the methodology section, the analyses were conducted in triplicate and the reported values are therefore averaged with the respective standard deviation. The components considered in this paper represent about 45 %wt of the RB, the rest of the mass of RB is made of carbohydrates and dietary fibres. Comparing the composition values obtained with those of other cultivars grown in Northern Italy (from Ferrara and Pavia) considerable similarity in the chemical composition can be observed (Petroni et al., 2017). This could be due to the similar weather conditions and cultivation techniques in those specific geographical areas. In fact, a comparison of the composition of the sample analysed in this work with that of a sample from a different geographical region (i.e. China) reveals more significant differences, particularly regarding proteins, fats and ashes contents (Qi et al., 2015). After the RB chemical characterization, and the quantification of the total fat content, the $SCCO_2$ extraction was performed to recover the RBB from the RB matrix.

3.2. RBB extraction efficiency and characterization

$SCCO_2$ extraction is an effective technique for the selective recovery of non-polar compounds from various complex sources (Fraterrigo Garofalo et al., 2023). The RBB obtained from the RB starting matrix is composed for 99 %wt of lipids. The chemical analysis revealed that 78 % in mass of the RBB material was oleic acid, while the content of waxes, estimated via GC-FID, was around 0.12 % m/m. The total amount of RBB obtained after the $SCCO_2$ Extraction was 796 g from a total of 13.03 kg of RB processed. Considering the amount of lipid in RB (Table 2), the extraction yield with $SCCO_2$ was around 42.8 %.

The fatty acids (FAs) composition of RBB is reported in Table 3; it is evident the high content of unsaturated FA, approximately 80 %wt of the total. Table 4 instead shows the triacylglycerides (TAG) composition of the RBB, together with the melting point and characteristic polymorphic structures of each TAG.

The main component of RBB is the monounsaturated oleic acid (42.4 % wt), followed by the polyunsaturated linoleic acid (35.1 %wt) and saturated palmitic acid (15.5 % wt) (Fraterrigo Garofalo et al., 2023). The free fatty acid analysis revealed that the 78 %wt was oleic acid. The high presence of unsaturated FAs is directly reflected in the TAGs profile. In fact, it can be observed that only around 6 %wt of the TAGs present are trisaturated (Table 4). The remaining portion shows at least one unsaturated chain in the TAG structure and consists mainly of TAGs composed by combinations of oleic and linoleic acid, as shown in Table 4. Due to their content of mono- and polyunsaturated fatty acids, vegetable oils with high content of unsaturated TAGs offer a lot of health benefits and valuable functional properties, making them highly relevant for food applications. Particularly, it has been demonstrated that the consumption of these types of products can reduce the risk of cardiovascular diseases by lowering the LDL cholesterol levels in the bloodstream (Lunn & Theobald, 2006).

The thermal behaviour of RB was initially investigated with DSC. Fig. 2 shows the thermograms recorded during heating and cooling of the extracted RBB. Upon heating, a small endothermic peak can be noticed at a temperature above 50°C, which correspond to the melting of the rice wax.

The melting of the other components (e.g., TAGs) generated broad melting peaks with onset at ambient temperature and final melting temperature at around 40°C. The recrystallization of the wax is visible during cooling, where a small exothermic peak at around 45°C is detected. The remaining RBB components crystallize below 30°C, where multiple peaks exothermic peaks are present, indicating the formation of several polymorphic structures.

The crystallization behaviour of RBB was further analysed using synchrotron SAXS and WAXS. These techniques enable the identification of different immiscible phases and the determination of their melting point and relative stability. Fig. 3**a** and Fig. 3**b** show the SAXS and WAXS patterns at 25°C, for samples after equilibration for several days. From the SAXS region, five different lamellar phases can be detected. The d-spacings were found to be the typical of 2 L and 3 L polymorphs, considering the average chain length of the RBB's TAGs. Although it is not possible to clearly detect all the five phases in the WAXS region it is evident the presence of β' polymorphs (orthorhombic), possibly

Table 2
comparison of obtained RB chemical composition and RB composition of other Northen Italy cultivars.

	Obtained Average Value [%wt]	Average Values from Italian Cultivars (Petroni et al., 2017) [%wt]	Average Values from Chinese Cultivar (Qi et al., 2015) [%wt]
Moisture	8.11 ± 0.06	9.11 ± 0.32	7.40 ± 0.02
Proteins	13.73 ± 0.28	12.40 ± 0.95	21.2 0± 1.6
Lipids	14.27 ± 1.04	19.08 ± 0.90	20.10 ± 0.50
Ashes	8.36 ± 0.10	8.86 ± 0.89	4.90 ± 0.02
Others	55.53 ± 0.37	50.55 ± 2.27	46.40 ± 2.1

Table 3
FAs' profile of RBB.

Fatty Acid	Average Value [%wt]
C14:0 Myristic Acid	0.27 ± 0.01
C16:0 Palmitic Acid	15.5 ± 0.5
C16:1 Palmitoleic Acid	0.13 ± 0.01
C18:0 Stearic Acid	0.13 ± 0.01
C18:1 Oleic Acid	42.4 ± 1.7
C18:2 Linoleic Acid (Omega-6)	35.1 ± 1.4
C18:3 γ-Linoleic Acid (Omega-6)	0.86 ± 0.03
C18:3 α-Linoleic Acid (Omega-3)	1.0 ± 0.03
C20:1 Eicosenoic Acid	0.58 ± 0.02
C22:0 Behenic Acid	0.96 ± 0.04
C20:3 Eicosatrienoic (Omega-6)	0.49 ± 0.01
C24:0 Lignoceric Acid	0.97 ± 0.04

Table 4
TAGs' profile of RBB with melting temperatures and existing polymorphic phases. P=palmitic acid, M=myristic acid, O=oleic acid, S=stearic acid, L=linoleic acid, Ln=linolenic acid.

Triglyceride	Average Value [%wt]	Melting Temperatures [°C] (Seilert et al., 2021)	Existing Phases (Seilert et al., 2021)
PPP	2.19	44.7, 56.6, 66.4	α, β', β
MOP	0.43	27	β
PPS	1.86	46.4, 58.7, 62.6	α, β', β
POP	2.38	16.6, 33.2 37.2	α, β', β
PLP	3.72		
MLO	2.12		
PSS	1.91	50.1, 61.8, 64.4	α, β', β
POS	1.53	19.6, 31	α, β
POO	8.2	18.5	β'
PLO	11.72		
PLL	6.05		
PLLn	0.2		
SOS	1.03	37, 41.5, 44	α, β', β
SOO	1.95	-1.6, 25.3	α, β'
SLS+OOO	8.25		
SLO	1.74		
OLO	20.74		
OLL	17.78		
LLL	5.9	-43,-12.9	α, β (Ravotti et al., 2020)
LLLn	0.3		

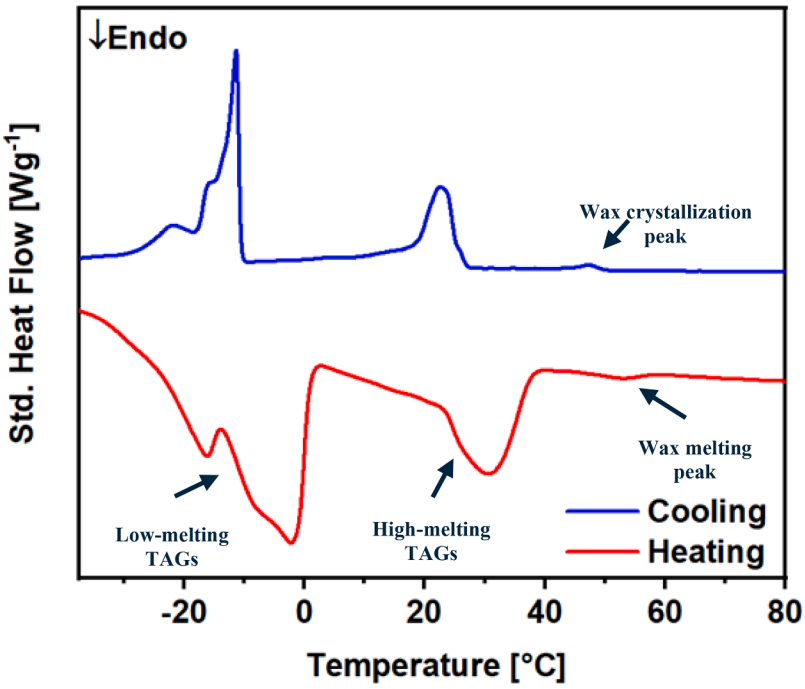

Fig. 2. DSC for RBB sample: thermal profiles recorded during heating (red) and cooling (blue) the sample.

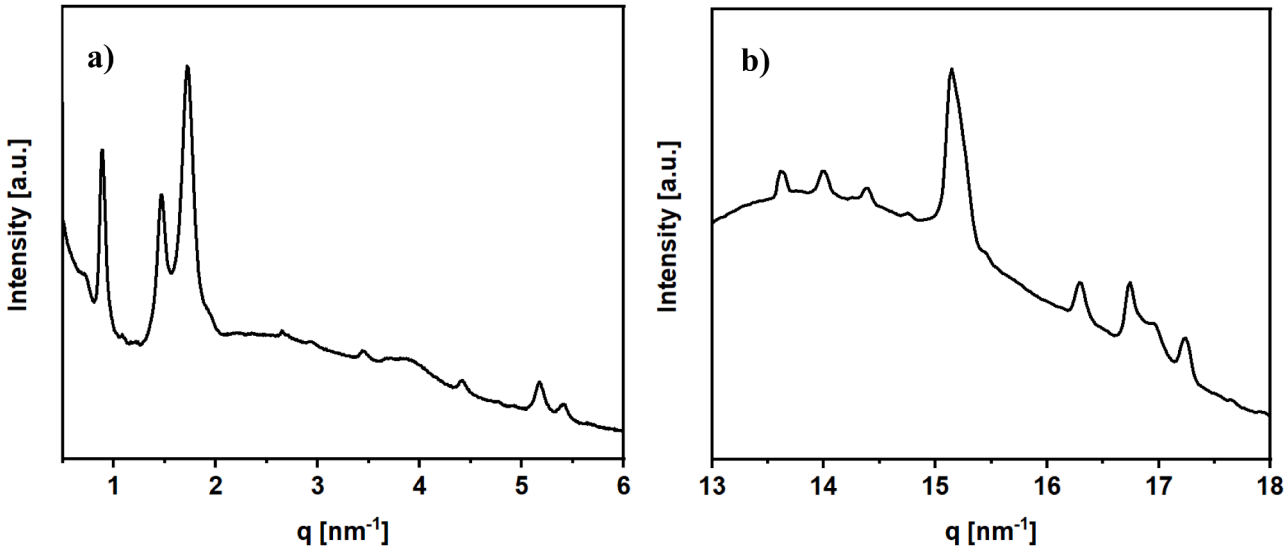

Fig. 3. Synchrotron X-Ray Diffraction patterns of RBB at equilibrium conditions (25°C): a)SAXS region and b)WAXS region.

associated with the rice bran wax. Further peaks are evident at high q, indicating the presence of β polymorphs. This would be consistent with the TAGs composition as trisaturated TAGs (e.g., PSS, PPP) can form β-2 L phases; whereas monosaturated (e.g., POP, SOS) are normally in β-3 L phases at equilibrium conditions. The main phases detected presented d-spacings of 7.2 nm and 6.4 nm, 5.3 nm and 5.8 nm, which are the β and β' phases of the RB TAGs and wax. Another peak at higher d-spacing of 8.50 nm was detected; nevertheless, due to its weak intensity it is not clear what polymorph it could be attributed to.

To better understand the polymorphic behaviour of RBB, SAXS and WAXS patterns were collected also during cooling (Fig. 4**a** and 4**b**) and heating (Fig. 4**c** and 4**d**) ramps. While cooling the sample, a first structure appeared at around 43°C, with a d-spacing of 7.2 nm (similar to the one observed at equilibrium conditions). Given the crystallization temperature (the highest among the other phases), it can be assumed that this phase is related to the wax fraction of the RBB, crystallizing in β' form.

Two other structures appeared below 25°C (at respectively 24.0°C and 19.5°C), with d-spacing of 6.9 nm and 7.6 nm, which correspond to another β' phase and possibly a γ-phase (lower intensity first peak) (Himawan et al., 2006). The equilibrium sample presented two more phases and slightly different d-spacing than those observed upon cooling; this indicates different stability of the phases observed (metastable vs stable), and possibly further crystallization and phase separation events happening at longer storage time.

A list of the forms observed upon cooling, including their melting points is reported in Table 5. The less stable phases are the first to melt below 40°C, while the melting temperature for the wax fraction is recorded at around 60°C.

As described in the methodology Section 2.5, RBB was preliminary

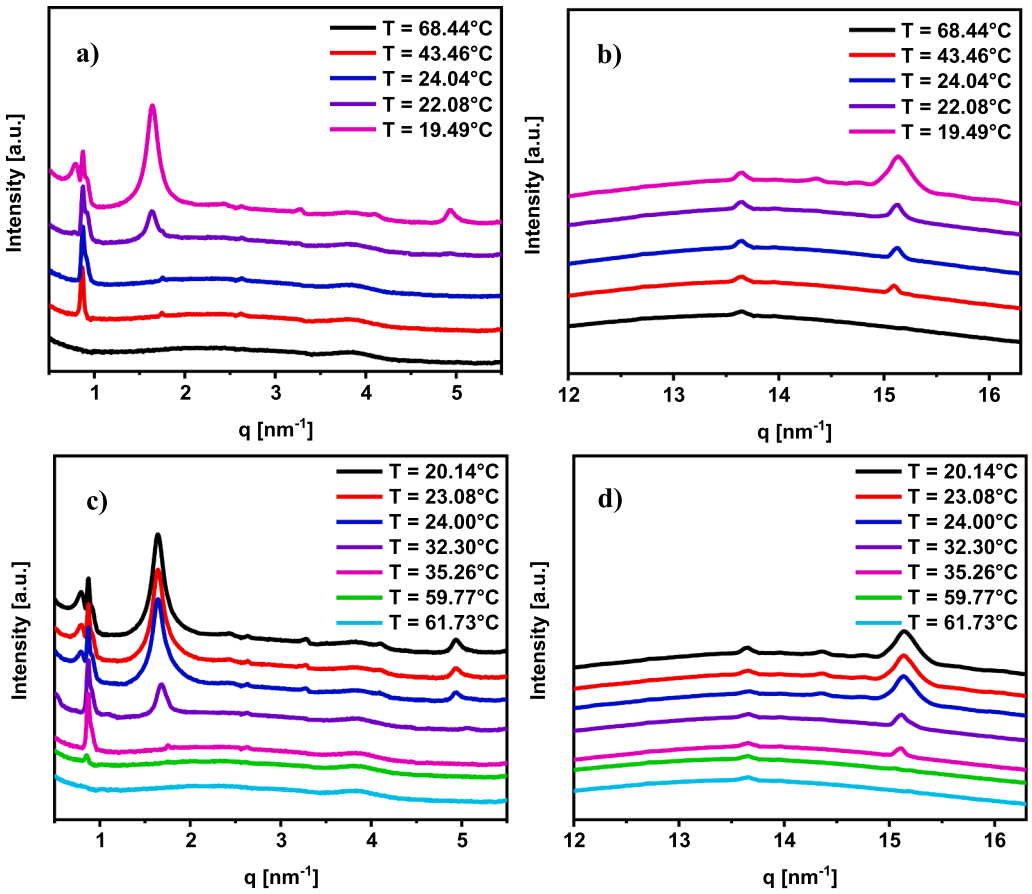

Fig. 4. Synchrotron X-Ray Diffractionpatterns of RBB with thermal ramps: a) SAXS region of RBB's diffractogram during the cooling step; b) WAXS region of RBB's diffractogram during the cooling step; c) SAXS region of RBB's diffractogram during the heating step; d) WAXS region ofRBB's diffractogram during the heating step.

Table 5
Calculated d-spacings for RBB's polymorphs appearing upon cooling.

	γ	β' (wax)	β'
q [nm-1]	0.76	0.87	0.91
	1.64	1.75	
	4.10	2.63	
d-spacing [nm]	7.61	7.16	6.89
Melting points [°C]	32.3°C	61.7°C	35.3°C

separated into its high melting wax (RBX) and lower melting oil fractions using different separation procedures not involving solvent extraction. At each purification step, a sample was collected for structural analysis. Specifically, the RBB sample was initially centrifuged, and the two resulting fractions (semi-solid and liquid) were collected. The semi-solid fraction was then filtered (with a sample also collected at this stage) and finally washed with ethanol (another sample was taken during this process as well). The crystallization behaviour of the obtained fractions was studied through synchrotron SAXS and the results are shown in Fig. 5. As the figure shows, comparing the results of the various purified samples, it is evident that the use of solvent improves the extraction of RBX from the starting matrix. The two lower melting phases identified upon cooling of the RBB sample (γ melting at 32.3°C with d-spacing of 7.6 nm and β' melting at 35.3°C with d-spacing of 6.9 nm) can be observed also during the cooling of the less pure semi-solid and oil fractions (Fig. 5**a, b** and **d**); whereas by better isolating the wax fractions (Fig. 5**c**) the higher melting phase of RBB (β' with 7.2 nm d-spacing) resulted the predominant one. Additional peaks, corresponding to the presence of residual lower melting TAGs were observed also in this relatively purer sample. In general, we can observe that the greater degree of wax purification, the higher the final melting temperature of the sample (up to more than 80°C). To better understand the polymorphic and thermal behaviours of RBX, a greater extent of purity is necessary. For this reason, the five purification strategies were developed and the results of the highly pure RBX isolated are presented in the next section.

3.3. RBX purification

As described in the methodology Section 2.5, five different processes involving solvent extraction have been developed for the isolation of RBX from RBB; these enable achieving a higher purity RBX fraction compared to the ones showed in Fig. 5, resulting from simple centrifugation, filtration and solvent washing operation. A comparison of them in terms of relative quantities of purified RBX extracted is shown in Table 6. The highest yields of material recovery were obtained through Process #2 and Process #5; in fact, Process #2 involved the highest number of unit operations employed, including four centrifugation steps, three melting and solvent addition steps and one vacuum filtration step (for a total of eight steps). The high extraction yield of Process #5 is probably related to the presence of a winterization step in the isolation procedure. Nevertheless, the filtration of winterized RBX might have entrapped some high melting TAGs in the wax crystals leading to a higher recorded weight; the presence of oil impurity is visible in the DSC thermogram of Fig. 7.

3.3.1. Purified RBX characterization

The first characterization technique performed on the extracted waxes was hot stage polarized light microscopy (PLM). With this set-up,

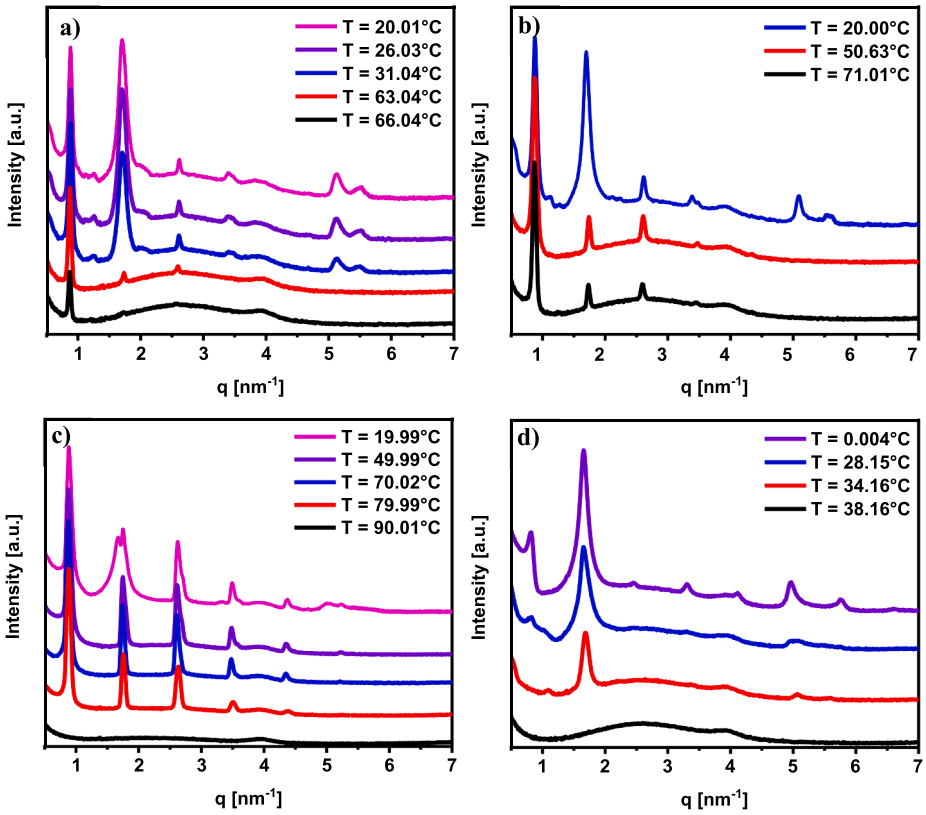

Fig. 5. SAXS regions of RBB's fraction with different extent of preliminary purification: a) Solid fraction after centrifugation; b) Solid fraction after centrifugation and vacuum filtration; c) Solid fraction after centrifugation, vacuum filtration, and ethanol washing; d) Liquid fraction after centrifugation.

Table 6
RBX extraction yields for different processes and different solvents.

	Solvent	Initial Weight (g)	Extracted Weight (g)	% Recovery
Process #1	Ethanol	22.48	0.11	0.47
	Isopropanol	21.90	0.10	0.43
Process #2	Ethanol	22.15	0.16	0.71
	Isopropanol	23.24	0.14	0.6
Process #3	Ethanol	25.02	0.06	0.24
	Isopropanol	24.02	0.05	0.21
Process #4	Ethanol	25.69	0.09	0.35
	Isopropanol	25.33	0.11	0.43
Process #5	Ethanol	22.38	0.15	0.65
	Isopropanol	21.98	0.15	0.68

the crystallisation and melting behaviour of RBX could be studied together with the sample microstructure. Fig. 6 shows the acquired images on three RBX samples extracted by using Process #2, #3 and #5 with EtOH as solvent (other images are available in the supporting information **Figure S6**). Some microstructural differences are visible among sample, but the morphology of the crystalline aggregates is similar as they were all needle like (of larger size in Process #5 RBX). This is in accordance with what observed by Toro-Vazquez et al. (2007) and Dassanayake et al., 2009.

The DSC analysis on the RBX samples were conducted as described in the methodology Section 2.7. The thermal behaviour of the purified waxes obtained with the various processes employed using IPA as solvent was analysed and the results are shown in Fig. 7. The results relative to the purification with EtOH are available in the supporting information **Figure S7.** From the thermograms, it is possible to appreciate the degree of purity achieved by each method presented. It can be seen that the processes consisting of more unit operations (e.g., Process #1 and Process #2) are those that provided RBX with narrower melting and crystallization peaks. In particular, the highest purity was achieved with Process #2 using IPA as extraction solvent. In general, it can be said that a higher energetic consumption, due to a higher number of unit operation steps included, provided a purer RBX, with narrower melting and more consistent crystallization temperatures. Furthermore, it is interesting to notice that the thermograms resulting from the RBX isolated through Process #5 show some clear extra melting peaks at temperatures between 50°C and 60°C. This might be related to the presence of entrained oil in the extracted wax crystals. Adding other unit operation steps in the downstream of Process #5 winterization step could completely isolate the relative RBX obtained, but a supplementary energetic cost should be also accounted. In all the cases, melting temperatures of around 80°C and crystallisation temperatures of around 77°C were recorded for the predominant RBX phase. This is consistent with the results reported also by Pandolsook & Kupongsak, 2020 for a similar wax material. These temperature ranges are typical of this type of recovered plant-based wax. Indeed, many commercially available RBX samples show similar values (77–82°C) but broader melting ranges (*Rice Bran Wax, 500 g High Hardness, Excellent Miscibility*, 2025). Having an ingredient with a narrow and specific melting point is fundamental for food or cosmetic industrial applications. In fact, this affects product stability and shelf-life and ensures greater reproducibility in the thermal and mechanical performance of the resulting formulations.

Based on the extraction yield and the degree of purity achieved, Process #2 was determined to be the best extraction method for RBX isolation. More trials were conducted to assess the reproducibility of this process, and the final yield value is 0.71 ± 0.06 % calculated from five trials. Therefore, this extract was the subject of a more detailed

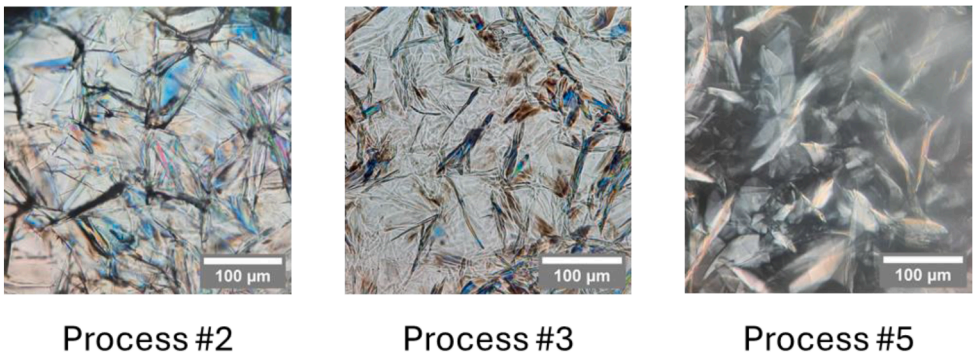

Fig. 6. PLM images of re-crystallized RBX obtained with different processes using ethanol as solvent.

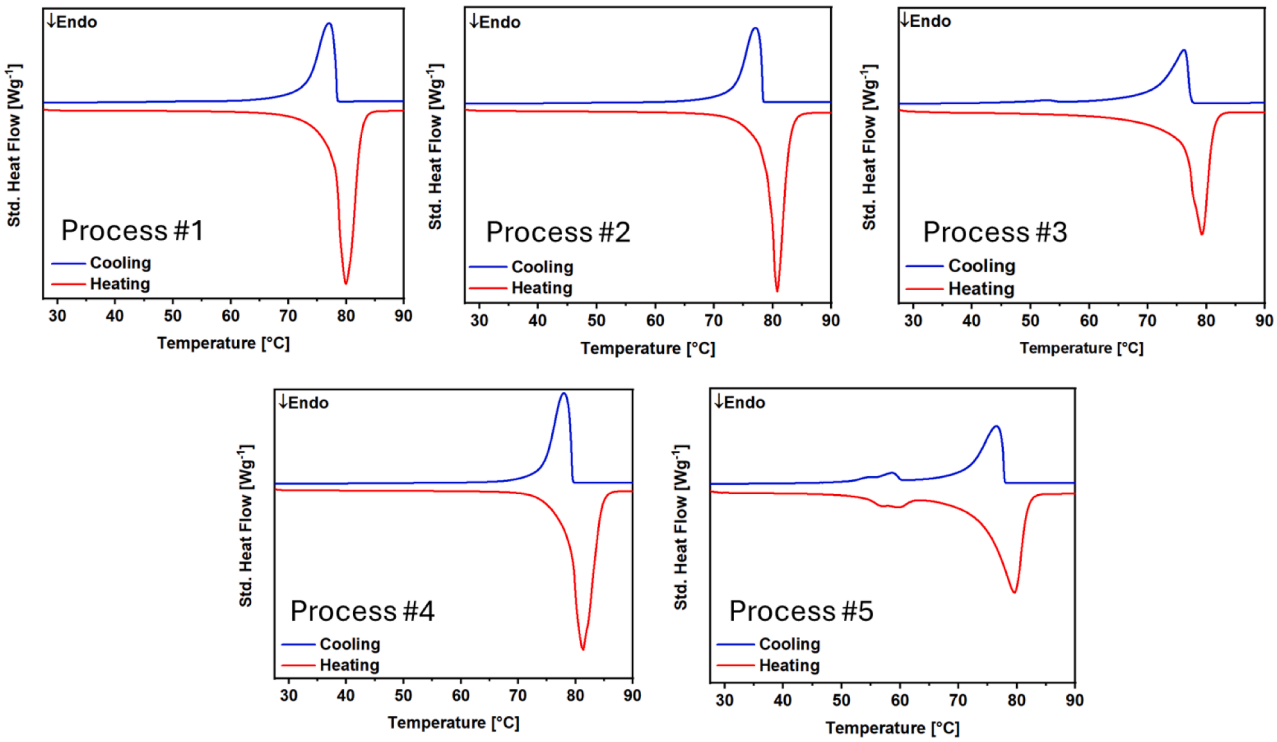

Fig. 7. DSC thermograms of RBX isolated with different purification processes using isopropanol as solvent.

structural analysis. Fig. 8 shows how the sample visual appearances immediately after the extraction and using PLM after re-crystallization. It can be observed that the isolated wax appears as white flakes. The image taken at 40x magnification under PLM after melting and recrystallization of RBX, shows the needle-like shape of the wax crystalline aggregates.

Fig. 8. Macroscopic appearance of extracted wax (Left); PLM images of re-crystallized RBX obtained with Process #2 (Right).

Synchrotron SAXS and WAXS (Fig. 9) were used to investigate the polymorphic behaviour of RBX extracted through Process #2 at equilibrium. The measurements conducted in the SAXS region provided information on the number of phases in the sample, their long-range stacking, of the wax molecules which is influenced by chain length, chain tilt, and the number of chains per layer (Schaink et al., 2007). These information are essential for product formulation as the affect product stability, rheological behaviour and texture.

It is evident from the SAXS pattern of Fig. 9 the presence of three different immiscible solid phases (I, II and III), which were not visible in the semi-purified sample of Fig. 5c.

Indeed, even for this sample these three phases are not clearly distinguishable in the WAXS region at ambient temperature, where three main peaks at d-spacings of 0.415, 0.372 and 0.296 nm can be observed and indicate an orthorhombic β'-polymorph sub-cell (Pandolsook & Kupongsak, 2020). Hence, dynamic experiments were conducted to study the RBX structural features during cooling (Fig. 10 **a and b**) and heating (Fig. 10 **c and d**) to better characterize the multiple phases present in this RBX sample. The d-spacings with the melting temperatures of the polymorphs identified upon cooling are reported in Table 7. The SAXS pattern of Fig. 10a show the formation of the three polymorphs detected at ambient temperature during cooling. The nucleation temperatures are between 78 and 70°C for the larger d-spacing forms, and around 60°C for the lower d-spacing one. Fig. 10**b** depicts the WAXS diffractograms of RBX during cooling from 90 to 25°C; similarly to what observed at ambient temperature, there are three distinct short-spacing peaks with d-spacings of 0.414 nm, 0.379 nm and 0.302 nm appearing at 77°C, and corresponding to an orthorhombic subcell.

However, shoulders with d-spacing around 0.375 nm are clearly visible in the WAXS region during cooling and confirm the presence of multiple β' polymorphs in the sample, in accordance with the SAXS region (Fig. 10a) (Ueno et al., 1997). It is worth noticing that, due to the wide range of temperature peaks of the same phase in both the WAXS and SAXS regions are observed shifting to higher q values during cooling; this is a common effect of temperature on crystalline structures (Sato et al., 1989).

Table 7 shows that two β' polymorph that nucleated at around 60°C showed a relatively lower melting point of around 63–64°C; whereas the other two structures melt fully at around 80°C.

In conclusion, it is evident that three high melting, orthorhombic β' phases characterize the RBX sample produced with process #2. The presence of multiple phases might be due to heterogeneous composition of the wax (e.g., different chain length molecules). Nevertheless, compared to the preliminary purified samples of Fig. 5 solvent extraction enables obtaining a product with narrower melting point and with lower TAGs contamination.

3.4. RBO characterization

The oil and solvent residues resulting from all tested extractions were stored and subsequently separated according to the methodology Section 2.6. The resulting product is solvent-free RBO. This was characterized through PLM and DSC analysis; the results are shown in Fig. 11. As can be seen under the PLM, during cooling the oil crystals grow in Maltese crosses spherulites (Acevedo & Marangoni, 2010). RBO crystallized at temperatures lower than room temperature (approximately 19°C), this is due to the high content of oleic acid in this fraction (which is characterized by β-polymorphic sub-cell at temperatures below 16°C (T. Editors of Encyclopaedia, 2024)).

After having extracted and characterized the presented RBB fractions, to understand the environmental impact and feasibility of the proposed separation methodologies a Life Cycle Assessment was conducted.

3.5. Life cycle assessment

The Life Cycle Assessment (LCA) evaluated and quantified the environmental impact of the five processes designed here for converting rice bran (RB) into rice bran wax (RBX) as the primary product and rice bran oil (RBO) as a co-product. These processes involved varying purification methods and two organic solvents: ethanol and isopropanol. The assessment was based on a functional unit (FU) of 1 kg of RBX, with impacts calculated using the ReCiPe 2016 MidPoint (H) method, which considers 18 impact categories (as reported in Table 8). Among the impact categories reported in Table 8, attention was focused on climate change and fossil sources depletion, as these allow for a direct assessment of how the results align with or deviate from the European Union's climate objectives. Specifically, the analysis is framed in the context of the European Green Deal's target of achieving net-zero emissions by 2050. Therefore, the study focused on the climate change impact category (Fig. 12), with other impact categories serving as supplementary indicators. Although specific policy targets for these additional categories are currently lacking, they nonetheless provide valuable contextual support for the interpretation of the results.

The LCA results are reported here by identifying the process configuration with the lowest environmental impact, determining the process step with the highest contribution, and comparing the environmental performance of configurations using ethanol (denoted as A) and isopropanol (denoted as B). Considering all the impact categories, among the five configurations, 2A_RBX reached the lowest impact, followed closely by 1A_RBX. In contrast, 5B_RBX achieved the highest

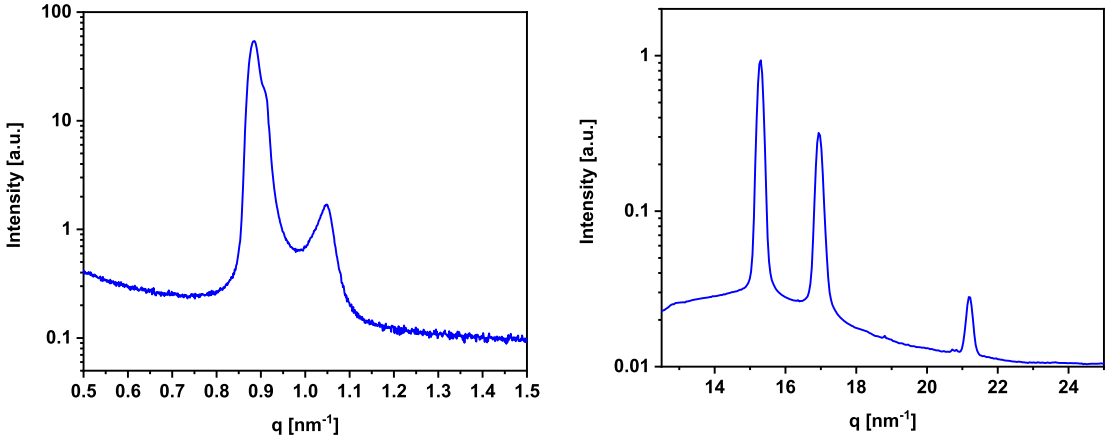

Fig. 9. RBX samples isolated with Process #2 diffractograms at static conditions (25°C): zoom of the SAXS (Left) and WAXS (Right) regions.

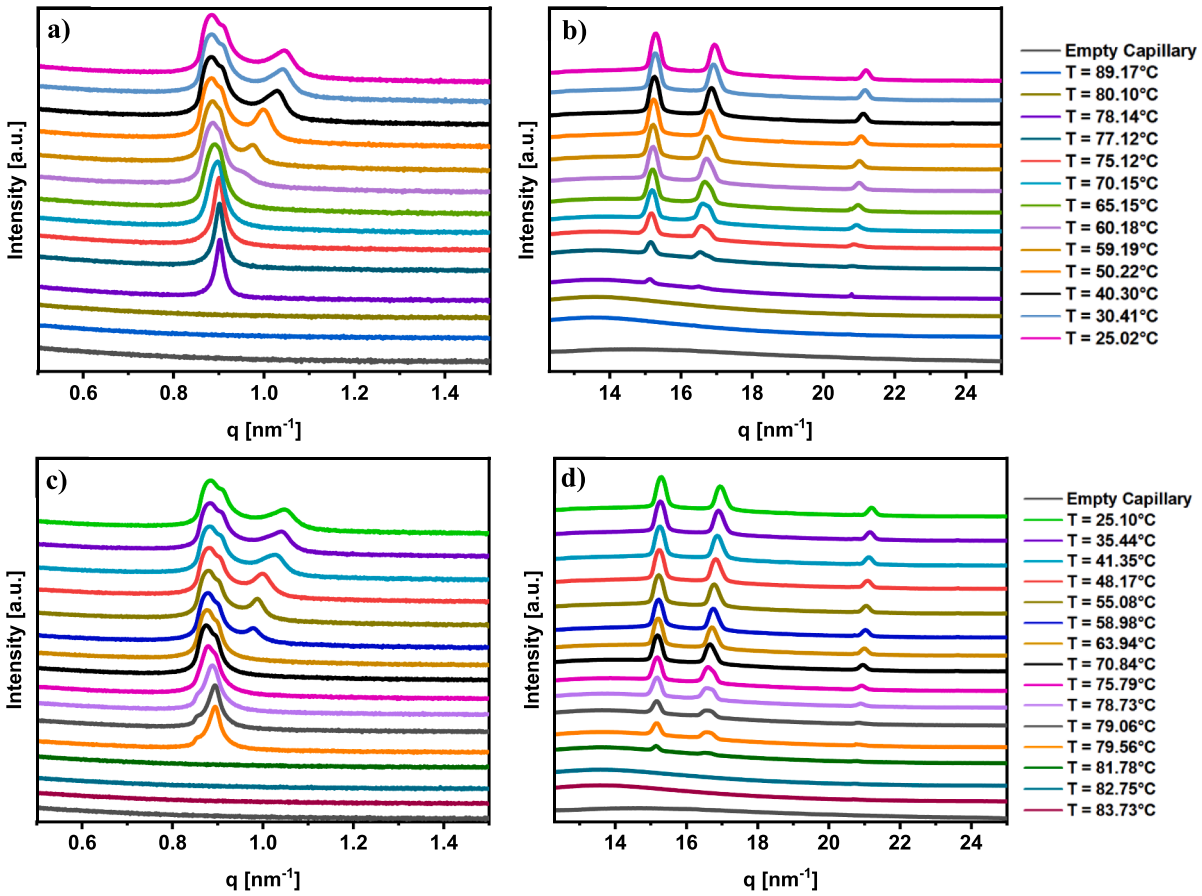

Fig. 10. RBX isolated with Process #2 diffractograms: a) SAXS region of the diffractogram during cooling; b) WAXS region diffractogram during cooling; c) SAXS region during heating; d) WAXS region during heating.

Table 7
q values, d-spacings for phases observed in RBX extracted with Process #2 (at 25°C) with their measured melting temperatures.

	I	II	III
q [nm^{-1}]	0.88 1.72 2.63	0.91	1.05 2.07
d-spacing [nm]	7.16	6.91	6.06
Melting points [°C]	82.75°C	81.78°C	63.94°C

impact. Across all configurations, the production of rice bran butter (RBB), the feedstock used for wax recovery, was identified as the most impactful step, contributing 70–85 % of the total climate change impact across all categories (Fig. 12).

The bottleneck in RBB production is the energy-intensive supercritical CO_2 extraction process, consistent with findings of De Marco et al., 2018 (De Marco et al., 2018). However, the energy consumption is offset by the benefits of supercritical CO_2, which minimizes solvent waste, leaves no residues, and allows the biomass to be processed without energy-intensive solvent removal, as reported in the study of Attard et al., 2018 (Attard et al., 2018). The bottleneck of energy-intensive processes can be faced by integrating renewable energy which can decrease carbon emissions and enhance energy efficiency. The National Renewable Energy Laboratory (NREL) (Denholm et al., 2022)(11) demonstrates that 100 % of clean electricity could be achieved by 2035 and can offer benefits that counterbalance the associated costs. Moreover, the Union of Concerned Scientists (Thoubboron, 2022) reported that renewable energy could help to reduce the electricity sector's emissions by around 81 %.

Configurations with higher wax yields require less RBB, reducing energy consumption during this step and consequently reducing environmental impacts. Purification is the second impactful step, influenced by two key factors: energy consumption and solvent used (type and amount).

Configuration 2A achieved the best environmental performance, combining the highest wax yield (7.10×10^{-3} g RBX/g RBB) with low energy consumption. This resulted in an overall impact of 88.1 kg CO_2 eq/FU.

Despite achieving the second and third-highest wax recovery yields ($6.81 \cdot 10^{-3}$ and $6.23 \cdot 10^{-3}$ g RBX/g RBB, respectively), configurations 5A and 5B had the highest energy demands due to cooling periods (36 hours) and high solvent use (10 ml of solvent/g of precipitate). These configurations recorded 94.38 and 90.76 kg CO_2 eq/FU impacts, respectively.

It is of interest to note that, configurations 3A and 3B reached the lowest wax yields ($2.40 \cdot 10^{-3}$ and $2.10 \cdot 10^{-3}$ g RBX/g RBB, respectively), but they required the least energy due to a simplified purification process involving only one melting step, their impacts were 88.6 and 90.8 kg CO_2 eq/FU, respectively.

Another important observation concerns the type of solvent used in the purification step. Across all configurations, the configurations using ethanol resulted in lower environmental impacts compared to the ones using isopropanol. According to the Ecoinvent 3.8 database, ethanol has

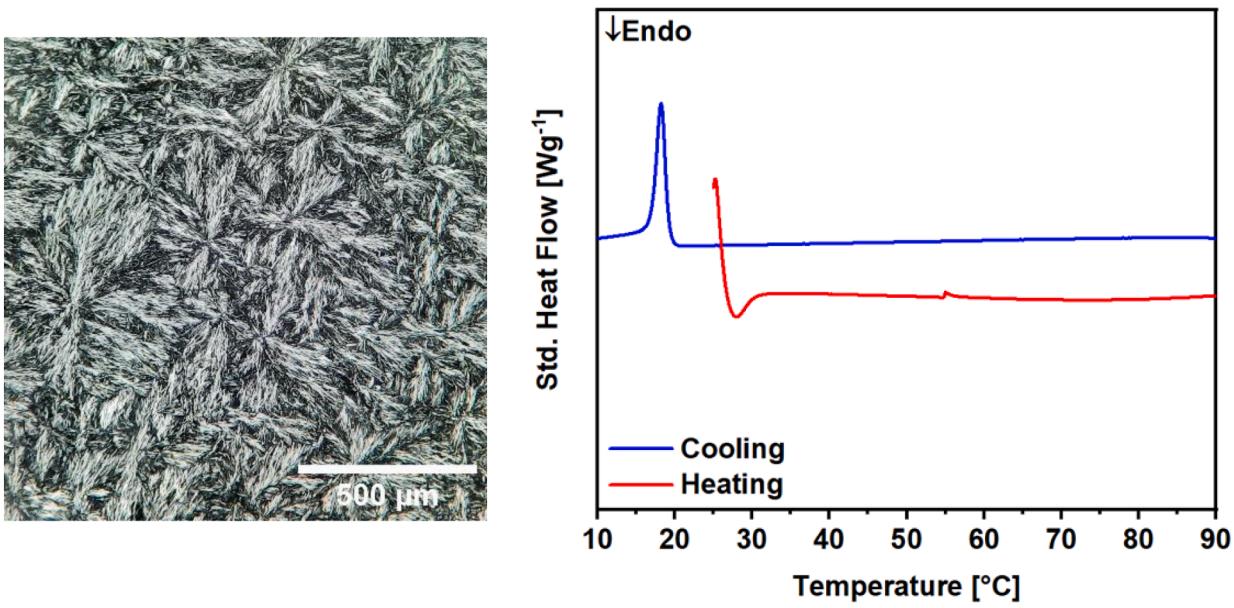

Fig. 11. PLM magnification of re-crystallized RBO (Left); DSC thermogram of RBO (Right).

Table 8
Environmental impacts calculated with ReCiPe 2016 MidPoint (H) and referring to the FU= 1 kg RBX. The elaboration was performed with the database Ecoinvent 3.8.5.

Impact categories	Unit	1A_RBX	1B_RBX	2A_RBX	2B_RBX	3A_RBX	3B_RBX	4A_RBX	4B_RBX	5A_RBX	5B_RBX
Global warming	kg CO2 eq	88.51	90.72	88.10	89.79	88.59	90.84	88.47	89.71	90.76	94.38
Stratospheric ozone depletion	kg CFC11 eq	5.59E-05	5.63E-05	5.57E-05	5.60E-05	5.58E-05	5.62E-05	5.59E-05	5.59E-05	5.51E-05	5.59E-05
Ionizing radiation	kBq Co-60 eq	10.74	10.90	10.73	10.84	10.72	10.88	10.74	10.81	10.60	10.91
Ozone formation. Human health	kg NOx eq	0.15	0.15	0.15	0.15	0.15	0.15	0.15	0.15	0.16	0.16
Fine particulate matter formation	kg PM2.5 eq	0.09	0.10	0.09	0.09	0.09	0.10	0.09	0.09	0.09	0.10
Ozone formation. Terrestrial ecosystems	kg NOx eq	0.15	0.16	0.15	0.16	0.15	0.16	0.15	0.15	0.16	0.17
Terrestrial acidification	kg SO2 eq	0.28	0.28	0.28	0.28	0.28	0.28	0.28	0.28	0.28	0.29
Freshwater eutrophication	kg P eq	0.02	0.02	0.02	0.02	0.02	0.02	0.02	0.02	0.02	0.02
Marine eutrophication	kg N eq	0.00	0.00	0.00	0.00	0.00	0.00	0.00	0.00	0.00	0.00
Terrestrial ecotoxicity	kg 1.4-DCB	74.30	78.51	73.59	76.88	74.57	78.98	74.09	77.01	83.65	90.04
Freshwater ecotoxicity	kg 1.4-DCB	1.06	1.09	1.06	1.07	1.07	1.09	1.06	1.07	1.16	1.19
Marine ecotoxicity	kg 1.4-DCB	1.47	1.51	1.46	1.48	1.47	1.51	1.46	1.48	1.59	1.64
Human carcinogenic toxicity	kg 1.4-DCB	2.28	2.32	2.26	2.29	2.28	2.32	2.27	2.29	2.37	2.42
Human non-carcinogenic toxicity	kg 1.4-DCB	35.97	36.70	35.76	36.29	36.03	36.78	35.95	36.28	37.28	38.32
Land use	m2a crop eq	2.03	2.05	2.02	2.03	2.04	2.05	2.04	2.03	2.04	2.06
Mineral resource scarcity	kg Cu eq	0.07	0.07	0.07	0.07	0.07	0.07	0.07	0.07	0.08	0.08
Fossil resource scarcity	kg oil eq	28.37	29.41	28.18	28.95	28.42	29.50	28.30	28.95	30.94	32.43
Water consumption	m3	1.53	1.55	1.53	1.54	1.53	1.54	1.53	1.53	1.54	1.56

a lower impact (1.24 kg CO_2 eq/kg) than isopropanol (2.01 kg CO_2 eq/kg).

The key factors influencing the process for the five configurations were consistent across other impact categories. Specifically, the ranking of configurations concerning environmental impact remained unchanged for fossil resource scarcity (measured in kg oil eq/FU), primarily driven by energy consumption. Configuration 2A achieved the lowest fossil resource scarcity, while configurations 5A and 5B had the highest. Similarly, for terrestrial ecotoxicity (measured in kg 1,4-DCB), configurations 5A and 5B recorded the highest impacts due to their significant solvent usage.

Furthermore, the sensitivity analysis (Table 9) provided additional insights, demonstrating that even considering a 5 % reduction in wax yield, the ranking of configurations remained unchanged. This highlights the significant contribution of energy consumption and solvent usage to the overall impact. This is because a 5 % decrease in wax yield requires processing approximately 5 % more feedstock than what was considered in the original LCA to produce 1 kg of RBX (the FU of the study). As a result, both the energy demand for the extraction process and the quantity of solvents used increase accordingly. The quantity of solvent required is directly proportional to the amount of feedstock processed, as the biomass-to-solvent ratio is kept constant. Additionally, the sensitivity analysis confirmed the robustness and consistency of the results.

To the best of the author's knowledge, no studies currently exist in the scientific literature regarding the environmental impacts of wax production from rice bran butter. However, this topic could be of interest, particularly considering existing research on wax extraction from barley straw (R. Sun & Sun, 2001), rice straw (Xiao et al., 2001), and rice bran (Vali et al., 2005) using conventional Soxhlet techniques. These techniques often involve solvents such as toluene, chloroform, petroleum ether, dichloromethane, and hexane. The use of these solvents raises environmental concerns due to their classification as volatile organic compounds (VOCs). VOCs contribute to air pollution by forming

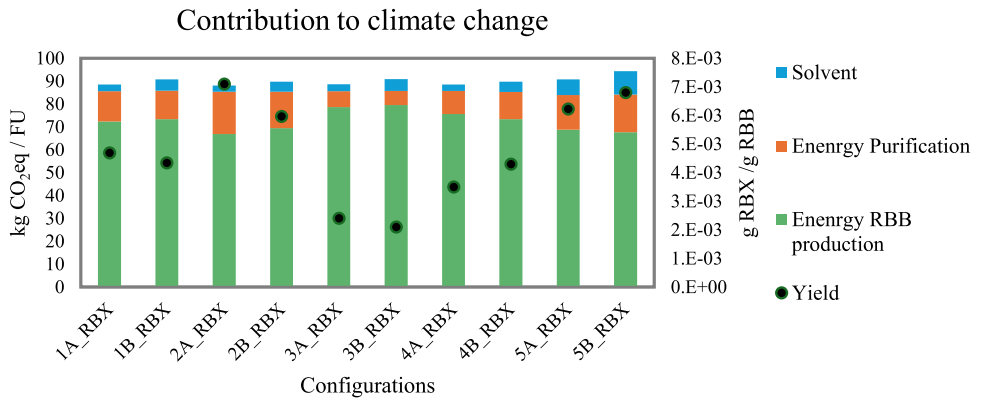

Fig. 12. Global warming, as a climate change impact category, considers the contributions from RBB production (primarily driven by energy consumption) and purification (influenced by both energy and solvent use). The wax yield is reported to highlight the relationship between technical performance and environmental impact.

Table 9
Environmental impacts calculated with ReCiPe 2016 MidPoint (H) and referring to the FU= 1 kg RBX. The elaboration was performed with the database Ecoinvent 3.8.5. The results refer to the sensitivity analysis where wax yield was considered to reduce to -5 %w/w.

Impact categories	Unit	1A_RBX	1B_RBX	2A_RBX	2B_RBX	3A_RBX	3B_RBX	4A_RBX	4B_RBX	5A_RBX	5B_RBX
Global warming	kg CO2 eq	91.61	93.89	91.19	92.93	91.69	94.02	91.57	92.85	93.93	97.68
Stratospheric ozone depletion	kg CFC11 eq	0.00	0.00	0.00	0.00	0.00	0.00	0.00	0.00	0.00	0.00
Ionizing radiation	kBq Co-60 eq	11.12	11.28	11.10	11.22	11.10	11.26	11.11	11.19	10.97	11.29
Ozone formation. Human health	kg NOx eq	0.16	0.16	0.15	0.16	0.16	0.16	0.15	0.16	0.16	0.17
Fine particulate matter formation	kg PM2.5 eq	0.10	0.10	0.10	0.10	0.10	0.10	0.10	0.10	0.10	0.10
Ozone formation. Terrestrial ecosystems	kg NOx eq	0.16	0.16	0.16	0.16	0.16	0.16	0.16	0.16	0.17	0.17
Terrestrial acidification	kg SO2 eq	0.29	0.29	0.28	0.29	0.29	0.29	0.29	0.29	0.29	0.30
Freshwater eutrophication	kg P eq	0.02	0.02	0.02	0.02	0.02	0.02	0.02	0.02	0.02	0.03
Marine eutrophication	kg N eq	0.00	0.00	0.00	0.00	0.00	0.00	0.00	0.00	0.00	0.00
Terrestrial ecotoxicity	kg 1.4-DCB	76.90	81.25	76.16	79.57	77.18	81.75	76.69	79.71	86.58	93.19
Freshwater ecotoxicity	kg 1.4-DCB	1.10	1.13	1.09	1.11	1.10	1.13	1.10	1.11	1.20	1.23
Marine ecotoxicity	kg 1.4-DCB	1.52	1.56	1.51	1.54	1.52	1.56	1.52	1.54	1.65	1.70
Human carcinogenic toxicity	kg 1.4-DCB	2.36	2.40	2.34	2.37	2.36	2.40	2.35	2.37	2.45	2.50
Human non-carcinogenic toxicity	kg 1.4-DCB	37.22	37.98	37.01	37.56	37.29	38.06	37.21	37.55	38.58	39.66
Land use	m2a crop eq	2.10	2.12	2.09	2.10	2.11	2.12	2.11	2.10	2.11	2.13
Mineral resource scarcity	kg Cu eq	0.07	0.08	0.07	0.07	0.07	0.08	0.07	0.07	0.08	0.08
Fossil resource scarcity	kg oil eq	29.37	30.44	29.17	29.96	29.41	30.53	29.29	29.96	32.02	33.56
Water consumption	m3	1.58	1.60	1.58	1.59	1.58	1.60	1.58	1.59	1.59	1.62

ground-level ozone and smog released into the atmosphere. Additionally, they pose significant risks to soil and water systems through long-term contamination. Their toxicity to aquatic organisms and potential persistence in water systems further underscores their environmental and human health risks. The low environmental impact of green extraction compared to the conventional ones is supported by the study of Aslanbay Guler et al. (2024), which investigated the environmental impacts of green extraction techniques for obtaining microalgal metabolites.

The findings of this study regarding the impact of climate change and fossil resource consumption are consistent with those reported by Sun et al., 2022, who investigated rice bran oil recovery. Sun et al., 2022 highlighted that the oil refining stage posed the most significant environmental impact, followed by the oil extraction stage, primarily due to high electricity demands. As mentioned earlier regarding the $SCCO_2$ step, Sun et al., 2022 proposed transitioning to renewable energy sources as a potential solution to replace traditional fuels, thereby contributing to the sustainable development of the industry. In this study, the LCA highlights that the optimal process configuration balances wax yield, energy consumption, and solvent use. Configuration 2A emerged as the most sustainable option, achieving the highest technical performance with the lowest environmental impact. This underscores the importance of efficient purification techniques and selecting low-impact solvents in minimizing the overall environmental burden of RBX production.

4. Conclusions

The valorisation of agri-food residues is a crucial element in the transition to sustainable economic systems. The extraction of high-value materials is an effective strategy for achieving this goal. The work presented here aimed to understand how to transform a rice industry non-primary product (RB) generally destined to be wasted into a high-value resource. A combination of $SCCO_2$ and green solvent extraction processes was used for the valorisation of RB via extraction of its lipidic fraction (RBB) and isolation of high-value rice bran wax (RBX) from it. The FA profile of RBB revealed a predominance of unsaturated fatty acids, with oleic (42.4 wt %) and linoleic acids (35.1 wt %) as major components. Structural and thermal analysis of RBB revealed the presence of a wax phase mixed with trisaturated, mono and polyunsaturated lower melting TAGs. The RBX fraction was isolated via five different purification strategies. Among these, Process #2 was found to be able to recover RBX with higher extraction yields compared to the others. This process involved the highest number of unit operations, in particular four centrifugation steps, three re-melting and solvent addition steps and one vacuum filtration step for a total of eight steps. The resulting wax was characterized by a melting point of around 80°C and a high degree of purity (e.g., low contamination from TAGs or FA). Nevertheless, three similar but immiscible orthorhombic β' and γ phases were detected in the RBX using X-ray scattering, probably associated to the presence of different wax molecules in the sample (e.g., different chain

lengths). Purity is fundamental when thinking about possible applications as a food ingredient or a pharmaceutical excipient. This property is crucial for obtaining products with reproducible and well defined thermal and mechanical performance as well as thermodynamic stability, ensuring a batch-to-batch reproducibility and minimising variability in the final products. Finally, a Life Cycle Assessment was carried out and highlighted that configuration 2A is the most sustainable of the different tested processes. In fact, configuration 2A achieved the highest technical performance with the lowest environmental impact because it balanced wax yield, energy consumption, and solvent use. LCA underlined the importance of selecting technically efficient purification techniques and low-impact solvents by minimizing the overall environmental impact of RBX production. This study supports the sustainable valorisation of rice bran wax through green extraction methods, yielding high-purity material with potential for food and cosmetic applications. A natural progression of this work is to try to reproduce the results obtained (particularly with the most efficient configuration 2A) with a pilot-scale plant for the production of larger RBX quantities. Pilot-plant studies can enable process optimization and to assess the effective solvent recovery. Additionally, including some economic considerations based on pilot-plant data could pave the way for an effective industrial-scale implementation of the proposed processes and future use of the extreme pure RBX obtained in industrial context.

CRediT authorship contribution statement

Danilo Candela: Writing – original draft, Visualization, Investigation, Formal analysis, Data curation, Conceptualization, Methodology, Validation, Writing – review & editing. **Janine Preston:** Investigation, Formal analysis, Conceptualization, Data curation, Validation. **Cecilia Fiore:** Writing – review & editing, Methodology, Investigation, Formal analysis, Data curation, Conceptualization. **Emmanuele Parisi:** Writing – review & editing, Methodology, Investigation, Formal analysis, Data curation. **Silvia Fraterrigo Garofalo:** Writing – review & editing, Investigation, Conceptualization, Data curation, Formal analysis, Methodology, Validation. **Francesca Demichelis:** Writing – review & editing, Writing – original draft, Methodology, Investigation, Formal analysis, Conceptualization, Data curation, Validation, Visualization. **Debora Fino:** Resources, Funding acquisition. **Elena Simone:** Writing – review & editing, Supervision, Resources, Funding acquisition, Conceptualization, Data curation, Project administration.

Declaration of competing interest

The authors declare that they have no known competing financial interests or personal relationships that could have appeared to influence the work reported in this paper.

Acknowledgements

We acknowledge Diamond Light Source (DLS) and CERIC for beamtime on beamlines I22 and SAXS under proposals SM34844–1 and SM37870 (DLS), 20242069, 20237090 and 20227148 (CERIC). Finally, we are grateful to beamline scientists Prof. Nick Terrill, Dr Andrew Smith and Dr Thomas Zinn (DLS), Dr Barbara Sartori and Dr Benedetta Marmiroli (CERIC, Elettra Sincrotrone Trieste) for the help and support with the two SAXS beamlines and special setups used for the work. Raw data collected on beamline I22 can be accessed from the main DLS repository. We are thankful to Marta Fontana for the help in collecting and analysing data on rice bran during her MSc project.

Data availability

Data will be made available on request.

References

Acevedo, N. C., & Marangoni, A. G. (2010). Characterization of the nanoscale in triacylglycerol crystal networks. *Crystal Growth and Design, 10*(8), 3327–3333. https://doi.org/10.1021/cg100468e

Aslanbay Guler, B., Tepe, U., & Imamoglu, E. (2024). Sustainable Point of View: Life Cycle Analysis for Green Extraction Technologies. *CBEN, 11*, 348–362. https://doi.org/10.1002/cben.202300056

Attard, T. M., Bukhanko, N., Eriksson, D., Arshadi, M., Geladi, P., Bergsten, U., Budarin, V. L., Clark, J. H., & Hunt, A. J. (2018). Supercritical extraction of waxes and lipids from biomass: A valuable first step towards an integrated biorefinery. *Journal of Cleaner Production, 177*, 684–698. https://doi.org/10.1016/j.jclepro.2017.12.155

Baldini, M., Fabietti, F., Giammarioli, S., Onori, R., Orefice, L., & Stacchini, A. (1996). *Analytical Methods Used In Food Control*.

Bas-Bellver, C., Barrera, C., Betoret, N., & Seguí, L. (2020). Turning agri-food cooperative vegetable residues into functional powdered ingredients for the food industry. *Sustainability, 12*(4). https://doi.org/10.3390/su12041284

Batuecas, E., Tommasi, T., Battista, F., Negro, V., Sonetti, G., Viotti, P., … Mancini, G. (2019). Life Cycle Assessment of waste disposal from olive oil production: anaerobic digestion and conventional disposal on soil. *Journal of Environmental Management, 237*, 94–102. https://doi.org/10.1016/j.jenvman.2019.02.021

Beccali, M., Cellura, M., Iudicello, M., & Mistretta, M. (2010). Life cycle assessment of Italian citrus-based products. Sensitivity analysis and improvement scenarios. *Journal of Environmental Management, 91*(7), 1415–1428. https://doi.org/10.1016/j.jenvman.2010.02.028

Butsat, S., & Siriamornpun, S. (2010). Antioxidant capacities and phenolic compounds of the husk, bran and endosperm of Thai rice. *Food Chemistry, 119*(2), 606–613. https://doi.org/10.1016/J.FOODCHEM.2009.07.001

Carbajal, D., Molina, V., Valdés, S., Arruzazabala, L., & Más, R. (1995). Anti-ulcer activity of higher primary alcohols of Beeswax. *Journal of Pharmacy and Pharmacology, 47*(9), 731–733. https://doi.org/10.1111/j.2042-7158.1995.tb06732.x

Cherubini, F., Strømman, A. H., & Ulgiati, S. (2011). Influence of allocation methods on the environmental performance of biorefinery products - A case study. *Resources, Conservation and Recycling, 55*(11), 1070–1077. https://doi.org/10.1016/j.resconrec.2011.06.001

Clift, R., Doig, A., & Finnveden, G. (2000). The application of Life Cycle Assessment to Integrated Solid Waste Management. Part 1 - Methodology. *Process Safety and Environmental Protection, 78*, 279–287. https://doi.org/10.1205/095758200530790

Dassanayake, L. S. K., Kodali, D. R., Ueno, S., & Sato, K. (2009). Physical properties of rice bran wax in bulk and organogels. *JAOCS. Journal of the American Oil Chemists' Society, 86*(12), 1163–1173. https://doi.org/10.1007/s11746-009-1464-6

De Marco, I., Riemma, S., & Iannone, R. (2018). Life cycle assessment of supercritical CO2 extraction of caffeine from coffee beans. *Journal of Supercritical Fluids, 133*, 393–400. https://doi.org/10.1016/j.supflu.2017.11.005

Demichelis, F., Tommasi, T., Deorsola, F. A., Marchisio, D., Mancini, G., & Fino, D. (2022). Life cycle assessment and life cycle costing of advanced anaerobic digestion of organic fraction municipal solid waste. *Chemosphere, 289*, 133058. https://doi.org/10.1016/j.chemosphere.2021.133058

Denholm, P., Brown, P., Cole, W., Mai, T., Sergi, B., Brown, M., Jadun, P., Ho, J., Mayernik, J., McMillan, C., & Sreenath, R. (2022). *Examining supply-side options to achieve 100% clean electricity by 2035*. https://doi.org/10.2172/1885591

FAOSTAT. (2019). State of food and agriculture 2019 : Moving forward on food loss and waste reduction. *Food & Agriculture Org*. https://www.fao.org/family-farming/detail/en/c/1245425/.

Feed prices and markets. (2025, February 13). https://ahdb.org.uk/dairy/feed-prices-and-markets.

Fraterrigo Garofalo, S., Cavallini, N., Destefano, R., Micera, M., Cavagnero, C., Botto, A., Savorani, F., Tommasi, T., & Fino, D. (2023). Optimization of supercritical carbon dioxide extraction of rice bran oil and γ-Oryzanol using multi-factorial design of experiment. *Waste and Biomass Valorization, 14*(10), 3327–3337. https://doi.org/10.1007/s12649-023-02111-w

Fraterrigo Garofalo, S., Demichelis, F., Mancini, G., Tommasi, T., & Fino, D. (2022). Conventional and ultrasound-assisted extraction of rice bran oil with isopropanol as solvent. *Sustainable Chemistry and Pharmacy, 29*. https://doi.org/10.1016/j.scp.2022.100741

Fraterrigo Garofalo, S., Tommasi, T., & Fino, D. (2021). A short review of green extraction technologies for rice bran oil. In *Biomass conversion and biorefinery, 11* pp. 569–587). Springer Science and Business Media Deutschland GmbH. https://doi.org/10.1007/s13399-020-00846-3

Garba, U., Singanusong, R., Jiamyangyeun, S., & Thongsook, T. (2019). Extraction and utilisation of rice bran oil. A review. *La Rivista Italiana Delle Sostanze Grasse, XCVI*.

Ghisellini, P., Cialani, C., & Ulgiati, S. (2016). A review on circular economy: The expected transition to a balanced interplay of environmental and economic systems. *Journal of Cleaner Production, 114*, 11–32. https://doi.org/10.1016/j.jclepro.2015.09.007

Himawan, C., Starov, V. M., & Stapley, A. G. F. (2006). Thermodynamic and kinetic aspects of fat crystallization. *Advances in Colloid and Interface Science, 122*(1–3), 3–33. https://doi.org/10.1016/j.cis.2006.06.016. Issues.

International Organization for Standardization. (n.d.-a). *ISO 12966-2:2015: animal and vegetable fats and oils - Gas chromatography of fatty acid methyl esters- Part 4: determination by capillary gas chromatography*.

International Organization for Standardization. (n.d.-b). *ISO 12966-2:2017: animal and vegetable fats and oils - Gas chromatography of fatty acid methyl esters- Part 2: preparation of methyl esters*.

Ishaka, A., Imam, M. U., Mahamud, R., Zuki, A. B. Z., & Maznah, I. (2014). Characterization of rice bran wax policosanol and its nanoemulsion formulation. *International Journal of Nanomedicine, 9*(1), 2261–2269. https://doi.org/10.2147/IJN.S56999

Kim, J. S., & Godber, J. S. (2001). Oxidative stability and vitamin E levels increased in restructured beef roasts with added rice bran oil. *Journal of Food Quality, 24*(1), 17–26. https://doi.org/10.1111/j.1745-4557.2001.tb00587.x

Kordsmeier, M., Howard, L. R., Brownmiller, C., Proctor, A., & Hauer-Jensen, M. (2015). Isolation of gamma and delta tocotrienols from rice bran oil deodorizer distillate using flash chromatography. *JAOCS, Journal of the American Oil Chemists' Society, 92*(9), 1243–1252. https://doi.org/10.1007/s11746-015-2696-2

Kuk, M. S., & Dowd, M. K. (1998). Supercritical CO2 extraction of rice bran. *JAOCS, Journal of the American Oil Chemists' Society, 75*(5), 623–628. https://doi.org/10.1007/s11746-998-0075-y

Kumari, B., Tiwari, B. K., Hossain, M. B., Brunton, N. P., & Rai, D. K. (2018). Recent Advances on Application of Ultrasound and Pulsed Electric Field Technologies in the Extraction of Bioactives from Agro-Industrial By-products. In *Food and bioprocess technology, 11* pp. 223–241). Springer New York LLC. https://doi.org/10.1007/s11947-017-1961-9

Lehmann Industrie - Top Discharge Vertical Centrifuges. (n.d.). Retrieved February 18, 2025, from https://lehmann-industrie.de/en/top-discharge-vertical-centrifuges/.

Liu, S. X., & Mamidipally, P. K. (2005). Quality comparison of rice bran oil extracted with d-limonene and hexane. *Cereal Chemistry, 82*(2), 209–215. https://doi.org/10.1094/CC-82-0209

Lunn, J., & Theobald, H. E. (2006). The health effects of dietary unsaturated fatty acids. *Nutrition Bulletin, 31*(3), 178–224. https://doi.org/10.1111/j.1467-3010.2006.00571.x

Mariotti, F., Tomé, D., & Mirand, P. P. (2008). Converting Nitrogen into Protein—Beyond 6.25 and Jones' Factors. *Critical Reviews in Food Science and Nutrition, 48*(2), 177–184. https://doi.org/10.1080/10408390701279749

Min, B., McClung, A. M., & Chen, M. H. (2011). Phytochemicals and Antioxidant Capacities in Rice Brans of Different Color. *Journal of Food Science, 76*(1). https://doi.org/10.1111/j.1750-3841.2010.01929.x

Modupalli, N., Thangaraju, S., Naik, G. M., Rawson, A., & Natarajan, V. (2022). Assessment of physicochemical, functional, thermal, and phytochemical characteristics of refined rice bran wax. *Food Chemistry, 396*. https://doi.org/10.1016/j.foodchem.2022.133737

Mohd Esa, N., & Ling, T. B. (2016). By-products of rice processing: An overview of health benefits and applications. *Rice Research: Open Access, 4*(1). https://doi.org/10.4172/jrr.1000107

Mohidem, N. A., Hashim, N., Shamsudin, R., & Man, H. C. (2022). Rice for food security: Revisiting its production, diversity, rice milling process and nutrient content. In *Agriculture (Switzerland), 12*. MDPI. https://doi.org/10.3390/agriculture12060741

Nanua, J. N., McGregor, J. U., & Godber, J. S. (2000). Influence of high-oryzanol rice bran oil on the oxidative stability of whole milk powder. *Journal of Dairy Science, 83*(11), 2426–2431. https://doi.org/10.3168/jds.S0022-0302(00)75132-0

Neumann, M. A. (2003). X-Cell: A novel indexing algorithm for routine tasks and difficult cases. *Journal of Applied Crystallography, 36*(2), 356–365. https://doi.org/10.1107/S0021889802023348

Nikitha, M., & Natarajan, V. (2020). Properties of South-Indian rice cultivars: Physicochemical, functional, thermal and cooking characterisation. *Journal of Food Science and Technology, 57*(11), 4065–4075. https://doi.org/10.1007/s13197-020-04440-3

Pandolsook, S., & Kupongsak, S. (2020). Potential use of policosanol extract from Thai bleached rice bran wax as an organogelator. *Journal of Food Measurement and Characterization, 14*(4), 2078–2086. https://doi.org/10.1007/s11694-020-00455-8

Pereira, C. S. M., & Rodrigues, A. E. (2014). Ethyl Lactate Main Properties, Production Processes, and Applications. In F. Chemat, & M. Abert Vian (Eds.), *Alternative solvents for natural products extraction* (pp. 107–125). Springer. https://doi.org/10.1007/978-3-662-43628-8_6.

Perry, R. H., & Green, D. W. (2008). *Perry's chemical engineers' handbook* (8th ed.). McGraw-Hill.

Petroni, K., Landoni, M., Tomay, F., Calvenzani, V., Simonelli, C., & Cormegna, M. (2017). Proximate Composition, Polyphenol Content and Anti-inflammatory Properties of White and Pigmented Italian Rice Varieties. *Universal Journal of Agricultural Research, 5*(5), 312–321. https://doi.org/10.13189/ujar.2017.050509

Piccinno, F., Hischier, R., Seeger, S., & Som, C. (2016). From laboratory to industrial scale: a scale-up framework for chemical processes in life cycle assessment studies. *Journal of Cleaner Production, 135*, 1085–1097. https://doi.org/10.1016/j.jclepro.2016.06.164

Protection Agency, E. (2010). *Economic study of solvent recycling and treatment – final report*.

Qi, J., Yokoyama, W., Masamba, K. G., Majeed, H., Zhong, F., & Li, Y. (2015). Structural and physico-chemical properties of insoluble rice bran fiber: Effect of acid-base induced modifications. *RSC Advances, 5*(97), 79915–79923. https://doi.org/10.1039/c5ra15408a

Ravotti, R., Worlitschek, J., Pulham, C. R., & Stamatiou, A. (2020). Triglycerides as novel phase-change materials: A review and assessment of their thermal properties. *Molecules, 25*(23), 5572. https://doi.org/10.3390/molecules25235572

Rice Bran Butter. (2025). https://www.theplantguru.com/shop/butters/ricebran-butter.html.

Rice Bran Oil. (2025). https://www.amazon.com/rice-bran-oil/s?k=rice+bran+oil.

Rice Bran Wax, 500 *g* High hardness, excellent miscibility. (2025). https://www.dictum.com/en/waxes-dbg/rice-bran-wax-500-g-714197.

Rohman, A. (2014). Rice Bran Oil's Role in Health and Cooking. *Wheat and Rice in Disease Prevention and Health*, 481–490. https://doi.org/10.1016/B978-0-12-401716-0.00037-4

Ruen-Ngam, D. (2014). *Gamma-Oryzanol extraction from upland rice bran*. https://www.researchgate.net/publication/269275355.

Sahena, F., Zaidul, I. S. M., Jinap, S., Karim, A. A., Abbas, K. A., Norulaini, N. A. N., & Omar, A. K. M. (2009). Application of supercritical CO2 in lipid extraction - A review. *Journal of Food Engineering, 95*(2), 240–253. https://doi.org/10.1016/j.jfoodeng.2009.06.026

Sahini, M. G., & Mutegoa, E. (2023). Extraction, phytochemistry, nutritional, and therapeutical potentials of rice bran oil: A review. In *Phytomedicine plus, 3*. Elsevier B.V.. https://doi.org/10.1016/j.phyplu.2023.100453

Sanoja-Lopez, K. A., Loor-Molina, N. S., & Luque, R. (2024). Rice Waste Feedstocks: A Review of Alternatives for their Conversion into High-Value Added Products. *BioResources*, 1814–1843. https://doi.org/10.15376/biores.19.1Sanoja-Lopez

Sapwarobol, S., Saphyakhajorn, W., & Astina, J. (2021). Biological Functions and Activities of Rice Bran as a Functional Ingredient: A Review. In *Nutrition and metabolic insights, 14*. SAGE Publications Ltd. https://doi.org/10.1177/11786388211058559

Sato, K., Arishima, T., Wang, Z. H., Ojima, K., Sagi, N., & Mori, H. (1989). Polymorphism of POP and SOS. I. occurrence and polymorphic transformation. *Journal of the American Oil Chemists' Society, 66*(5), 664–674. https://doi.org/10.1007/BF02669949

Schaink, H. M., van Malssen, K. F., Morgado-Alves, S., Kalnin, D., & van der Linden, E. (2007). Crystal network for edible oil organogels: Possibilities and limitations of the fatty acid and fatty alcohol systems. *Food Research International, 40*(9), 1185–1193. https://doi.org/10.1016/j.foodres.2007.06.013

Seilert, J., Moorthy, A. S., Kearsley, A. J., & Flöter, E. (2021). Revisiting a model to predict pure triglyceride thermodynamic properties: Parameter optimization and performance. *JAOCS, Journal of the American Oil Chemists' Society, 98*(8), 837–850. https://doi.org/10.1002/aocs.12515

Serrano, S., Rincón, F., & García-Olmo, J. (2013). Cereal protein analysis via Dumas method: Standardization of a micro-method using the EuroVector Elemental Analyser. *Journal of Cereal Science, 58*(1), 31–36. https://doi.org/10.1016/j.jcs.2013.04.006

Singanusong, R., & Garba, U. (2019). Micronutrients in rice bran oil. *Rice bran and rice bran oil: chemistry, processing and utilization* (pp. 125–158). Elsevier. https://doi.org/10.1016/B978-0-12-812828-2.00005-6

Sookwong, P., & Mahatheeranont, S. (2017). Supercritical CO2 extraction of rice bran oil – the technology, manufacture, and applications. *Journal of Oleo Science, 66*(6), 557–564. https://doi.org/10.5650/jos.ess17019

Strieder, M. M., Pinheiro, C. P., Borba, V. S., Pohndorf, R. S., Cadaval, T. R. S., & Pinto, L. A. A. (2017). Bleaching optimization and winterization step evaluation in the refinement of rice bran oil. *Separation and Purification Technology, 175*, 72–78. https://doi.org/10.1016/j.seppur.2016.11.026

Sun, L. H., Wang, Y. Y., & Gong, Y. Q. (2022). Life cycle assessment of rice bran oil production: A case study in China. *Environmental Science and Pollution Research, 29*(26), 39847–39859. https://doi.org/10.1007/s11356-021-18172-0

Sun, R., & Sun, X.-F. (2001). Separation and characterization of lipophilic extracts from barley straw. *Separation Science and Technology, 36*(13), 3027–3048. https://doi.org/10.1081/SS-100107644

T. Editors of Encyclopaedia. (2024, January 31). *Oleic acid*. Encyclopedia Britannica. https://www.britannica.com/science/oleic-acid.

Tan, B. L., Norhaizan, M. E., & Chan, L. C. (2023). Rice Bran: From waste to nutritious food ingredients. In *Nutrients, 15*. MDPI. https://doi.org/10.3390/nu15112503

Thoubboron, K. (2022, November 2). *The advantages and disadvantages of renewable energy*. https://www.energysage.com/about-clean-energy/advantages-and-disadvantages-of-renewable-energy/.

Thushari, I., Vicheanteab, J., & Janjaroen, D. (2020). Material flow analysis and life cycle assessment of solid waste management in urban green areas, Thailand. *Sustainable Environment Research, 30*(1). https://doi.org/10.1186/s42834-020-00057-5

Tomita, K., Machmudah, S., Wahyudiono, Fukuzato, R., Kanda, H., Quitain, A. T., Sasaki, M., & Goto, M. (2014). Extraction of rice bran oil by supercritical carbon dioxide and solubility consideration. *Separation and Purification Technology, 125*, 319–325. https://doi.org/10.1016/j.seppur.2014.02.008

Toro-Vazquez, J., Morales, J., Dibildox-Alvarado, E., Charo, M., Alonzo-Macías, M., & González-Chávez, M. (2007). Thermal and Textural Properties of Organogels Developed by Candelilla Wax in Safflower Oil. *Journal of Oil & Fat Industries, 84*, 989–1000. https://doi.org/10.1007/s11746-007-1139-0

Tufail, T., Ain, H. B. U., Chen, J., Virk, M. S., Ahmed, Z., Ashraf, J., Shahid, N. U. A., & Xu, B. (2024). Contemporary views of the extraction, health benefits, and industrial integration of Rice Bran Oil: A prominent ingredient for holistic human health. In *Foods, 13*. Multidisciplinary Digital Publishing Institute (MDPI). https://doi.org/10.3390/foods13091305

Ueno, S., Minato, A., Seto, H., Amemiya, Y., & Sato, K. (1997). Synchrotron radiation X-ray diffraction study of liquid crystal formation and polymorphic crystallization of SOS (*sn* -1,3-Distearoyl-2-oleoyl Glycerol). *The Journal of Physical Chemistry B, 101*(35), 6847–6854. https://doi.org/10.1021/jp9715639

Vali, S. R., Ju, Y. H., Kaimal, T. N. B., & Chern, Y. T. (2005). A process for the preparation of food-grade rice bran wax and the determination of its composition. *JAOCS, Journal of the American Oil Chemists' Society, 82*(1), 57–64. https://doi.org/10.1007/s11746-005-1043-z

Xiao, B., Sun, X. F., & Sun, R. (2001). Extraction and characterization of lipophilic extractives from rice straw. I. chemical composition. *Journal of Wood Chemistry and Technology, 21*(4), 397–411. https://doi.org/10.1081/WCT-100108334

You, S. (2022). The waste challenge. *Waste-to-Resource System Design for Low-Carbon Circular Economy*, 1–8. https://doi.org/10.1016/B978-0-12-822681-0.00005-0

Yu, S., Nehus, Z. T., Badger, T. M., & Fang, N. (2007). Quantification of vitamin E and γ-oryzanol components in rice germ and bran. *Journal of Agricultural and Food Chemistry, 55*(18), 7308–7313. https://doi.org/10.1021/jf071957p

ZHENGZHOU GREATWALL Scientific Industrial and Trade Co., Ltd. - 10L Rotary Evaporator. (n.d.). Retrieved February 18, 2025, from https://gwsionline.com/10L-rotary-evaporator/.